



JÖNKÖPING UNIVERSITY  
*School of Engineering*

# Development of a complex robot structure

Development and analysis of a cast triple traction system for the robot  
operating at CERN facilities

**PAPER WITHIN** *Casting development*

**AUTHOR:** *Gerard Aliana Cervera*

**TUTOR:** *Jakob Olofsson / Luca Rosario Buonocore*

**JÖNKÖPING** January 2023

This exam work has been carried out at the School of Engineering in Jönköping in the subject area of cast pieces development and simulation. The work is a part of the Master of Science program. The authors take full responsibility for opinions, conclusions and findings presented.

Examiner: Nils-Eric Andersson

Supervisor: Jakob Olofsson / Luca Rosario Buonocore

Scope: 15 credits

Date: 07 March 2023

## **Abstract**

All devices working in hazardous environments have specific requirements to reduce the intervention of human power as much as possible. The robot that this thesis is focused on is no exception to this rule. This dissertation summarized the process followed to achieve a theoretical design of a traction system for the CERNBot, the robot that operates at CERN facilities.

This traction system had to be capable of achieving a speed of 10 km/h, going upstairs and make tight turns without draining completely the battery of the device. For that purpose, it was decided to include three types of traction systems such a pneumatic wheel, a track system and a mecanum-wheel (an omnidirectional wheel capable of moving in any direction). This design had to include as many commercially available pieces as possible to maintain the costs contained.

In order to comply and extend the battery lifetime as much as possible, topological optimization was applied to the non-commercial pieces, reducing the weight of the piece by 25%.

After achieving the weight reduction, a discussion about the best manufacturing methodology is done, comparing the manufacture using a CNC machine or casting the device, including the possible defects and costs that both models can have.

The results show that manufacturing this piece with casting can lead to a cheaper and more complex piece.

## Summary

This report explains the process followed to design a theoretical design of a traction system for the robot that does operational maintenance at CERN facilities.

It starts with a short introduction about the robot itself and where it will be operating, including the current traction system used in operation. The main goal was to achieve a manufacturable design adaptable to the current body of the robot and optimizing the non-commercial parts. After it, this thesis aimed to help choosing the manufacturing process for the structure.

In order to do so, and after selecting between different possible designs, the commercial components required were selected and the forces calculated. With those forces and relying on the help of CAE design tool like Ansys, a stress and deformation simulation was done in the structure of the system, followed by a topological optimization to reduce the weight.

Considering the complex shapes that a topological optimization can bring, a casting simulation (using MAGMAsoft 5.5.1) of this piece was done to observe the viability of using this methodology. Last but not least, the economical aspect is considered when compared with manufacturing it with CNC machining.

As found during this thesis, casting is considered to be the most economical way of manufacturing this piece.

### Keywords

CERNBot, Traction, Topology optimization, Sand casting

## Contents

1	Introduction.....	5
	1.1.1 The CERNBot.....	6
2	Theoretical background.....	9
	2.1 Product development.....	9
	2.2 Material selection.....	10
	2.3 Aluminium designation and characteristics .....	11
	2.4 Process selection.....	11
	2.4.1. Casting .....	12
	2.4.2. CNC machining.....	15
3	Problem description.....	16
	3.1. Concept design.....	16
	3.1.1. Technical requirements.....	16
	3.2. Forces applied.....	17
	3.3. Industrial components .....	20
4	Simulations .....	23
	4.1. Introduction to FEM analysis .....	23
	4.2. Mechanical simulations .....	23
	4.2.1. Mesh quality.....	24
	4.2.2. Simulation results .....	25
	4.3. Final models.....	27
	4.4. Casting simulation.....	29
	4.4.1. Cast geometry.....	29
	4.4.2. Simulation setup.....	33
	4.4.3. Results.....	34
5	Economic analysis.....	39
	5.1. CNC version cost.....	39
	5.2. Cast version cost.....	40
6	Conclusion.....	43
	6.1 Overall.....	43
	6.2. Further work.....	43
7	References.....	44

## Introduction

8	Search terms .....	46
9	Appendix 1 .....	47

## 1 Introduction

This report details the design challenge proposed by the European Organization for Nuclear Research (CERN), and how the different requirements and particularities have been addressed in order to approach a manufacturing and economic study of a triple traction system for the CERNBot, one of the robots that operates in the underground ( $\sim 120\text{m}$  deep) tunnels of the LHC and the other accelerators.

Included in the first section, a brief explanation will be presented, as an introduction, about the facilities where the project has been developed, the reasons behind this particular design and the project objectives. It will also present the robot and the requirements and limitations that this project will have.

### 1.1 Background

CERN is a European research organization that operates the largest particle physics laboratory in the world. The organization is based to the northwest of Geneva on the Franco-Swiss border and has 23 member states. It is also used to refer to the laboratory, with approximately 2,500 scientific, technical, and administrative staff members, and about 12,000 users (CERN, 2020).

Its main function is to provide and maintain the particle accelerators and other infrastructures needed for high-energy physics research. It operates a network of six accelerators and one decelerator. Each machine in the chain increases the energy of particle beams before delivering them to experiments or to the next, more powerful accelerator.

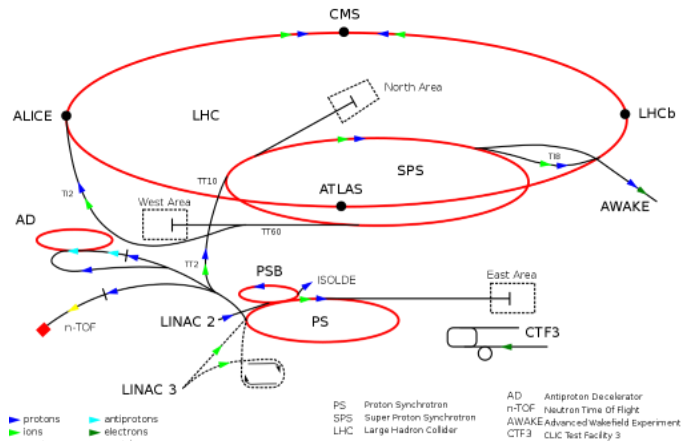


Figure 1 CERN facilities

These different particle accelerators connect between each other in different depths underground, which means that there are stairs, although they are in low radiation areas.

CERN's experiments involve colliding particles beams together or into a stationary target. When this happens some of the particles release radiation or new particles are created. Radiation only occurs when the particle beam is on, and turning it off stops the emissions immediately. Radiation is sometimes causing some of the components surrounding the collision points to become radioactive. These components are well confined and their handling is rigorously controlled.

Due to this radiation, and the danger related to the operation of the accelerators, the physical interventions done on the tunnels should be reduced. In order to reduce the human interventions, while keeping a correct maintenance and surveillance of the different areas, it was decided to use robotics.

## 1.1.1 The CERNBot

CERNBot(CERNbot | *Knowledge Transfer*, 2018) (see Figure 2) is a robotic platform developed at CERN for complex interventions in presence of hazards like ionization radiation.

The upper module can have two robotic arms installed and can be deployed into other mechanical structures (like TIM robot, another type that uses a rail to move along CERN tunnels and accelerators. The lower module allows the change of the type of wheel depending on the surface that the robot will be placed in, between mecanum-wheels (a type of omnidirectional wheel) and rubber wheels and a reduction of the battery depending on the weight requirements.

All these modular modifications need to be done by an operator at the surface before the operation starts. The work environment limits the interventions underground.

This makes for a very versatile robotic solution. In addition, the chassis is very stable and can be safely operated with two robotic arms installed on a lifting chariot. The whole platform uses standard industry components for most of mechanical, electronics and control components. This fact makes the robot really easy to upgrade in case it is needed. This also keeps the cost at a very competitive level for a platform with a payload of up to 250 kg.

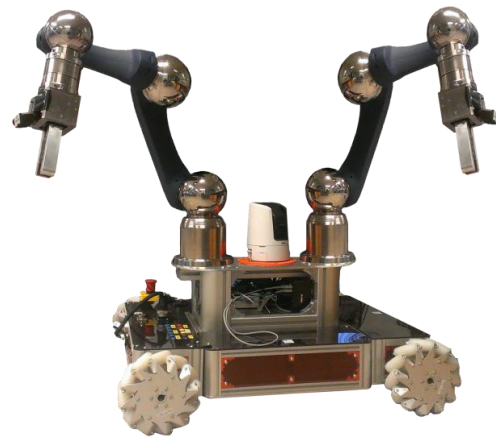


Figure 2 CERNBot (CERNbot | *Knowledge Transfer*, 2018) with commercial industrial arms mounted

This chassis has a dimension of 80 cm long per 50cm width and 30 cm tall if only the chassis is considered (60 including the arms base) or up to 2 meters with the arms fully extended

Another interesting fact about CERNBot is that it is a real-time operating system. Currently, this robot is being developed to recognize unconscious humans.

Advantages	Limitations
<ul style="list-style-type: none"> <li>• Highly versatile platform</li> <li>• High payload</li> <li>• Competitive cost base.</li> <li>• Standard industrial components</li> <li>• Employee exposure reduction.</li> <li>• Data-extraction from human inaccessible areas</li> </ul>	<ul style="list-style-type: none"> <li>• Current version does not support operations on harsh terrain.</li> <li>• Base weight of ~150 kg</li> <li>• Max speed of 10 km/h</li> </ul>

Table 1 Advantages and limitations of the current version of CERNBot



This robot main body (without considering the arms) is used as a base for other robots developed at CERN such as CERNBot, TIM or Marchese (Tvede, 2021). All the robots using this base are entirely controllable from ground level, user friendly with GUI and including a novel energy management system.

### **1.1.2. The product**

The idea behind this project is to develop a new traction system for the platform of the CERNBot. This traction system will combine mecanum-wheels, rubber wheels and tracks, avoiding the need of the operator to change them by hand.

This design is required due to the need of avoiding the human intervention when stairs are found and to increase the maneuverability without any external intervention.

The current method used when stairs are found is that two operators have to take the robot and place it in the upper (or lower) floor, in a flat surface area. From that point, the remote handling can continue. In the case of tight spaces, the robot requires a lot of time to reach the correct position or requires the intervention of a technician to place it properly.

## **1.2 Purpose and research questions**

The aim of this thesis work is to:

- Make a viable mechanical design for the traction system
- Calculate the forces the prototype will receive
- Optimize the non-commercial mechanical parts to reduce its weight
- Choose a casting process for the structure
- Choose an alloy material
- Design a gating system
- Show areas susceptible to defects
- Comparison with other methodologies

## **1.3 Delimitations**

The scope of this thesis is limited to the 3D model, the simulation of the mechanical design and casting process, focusing the conclusions on the final results and costs that this piece could have. This is achieved by comparing the results and approximate price of the proposed optimized solutions, adapted to different manufacturing systems.

This thesis did not include a physical trial production of the casting system nor any other manufacturing system and thus, comparison of simulation results with manufactured pieces is also out of the scope of this thesis.

## **1.4 Outline**

The main body of this report details the specifications of a traction system, including the different parts, and the simulations and calculations applied in order to reach it. After these mechanical calculations, a simulation into the casting methodology will be done, by selecting a process and material, modifying the piece to make it suitable for those selections and a simulation of the cast part.

Following this part, a brief economic analysis is done in order to compare this manufacturing technology with other available solutions.

## 2 Theoretical background

This chapter will introduce some of the concepts needed to achieve a correct design, as well as a proper material and manufacturing methodology for the design proposed in this thesis.

### 2.1 Product development

The encyclopedia of Production Engineering defines the product development as the creation of products with new characteristics that offer a new or additional benefit to the customer or user (Lutters, 2014) This development can involve the formulation of an entirely new product that satisfy the needs of a market niche, such as CERN, even if it is a really reduced niche.

This process can be simplified into in eight different phases (Lutters, 2014) such as:

1. Idea generation
2. Idea screening
3. Concept development and testing
4. Business analysis
5. Beta testing
6. Technical implementation
7. Commercialization
8. Product pricing

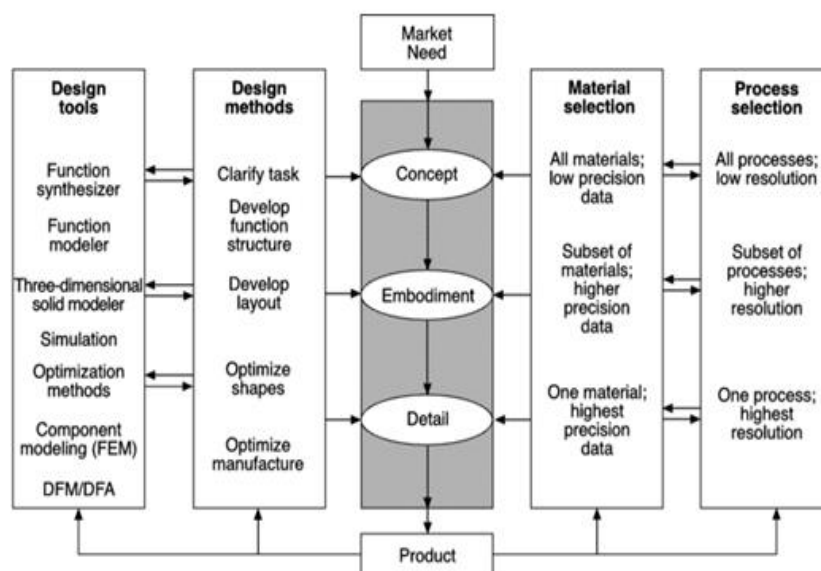


Figure 3 Schematic of the design process (Dieter, 1997)

The product development cycle has to be accompanied by an adequate requirement specification and can be reiterated as much as needed to perform accordingly. This thesis is focused on the concept development of this product.

## Theoretical background

This phase can be at the same time divided into 3 sub phases (Dieter, 1997) such as concept, embodiment and detail, each on with deeper complexity than the previous. All this complexity can be seen on Figure 3.

### 2.2 Material selection

The selection of a correct material for a design is a key step that links simulations and 3D design with reality.

All materials have different properties, making them more suitable for a certain function and/or process. The main properties that define a material for this project are the density, strength, rad-hazardous resistance and the associated cost.

In this case of study, the radiation produced on the tunnels when in contact with different materials brings changes in the viscosity, solubility, conductivity and the most important ones, tensile strength, hardness and flexibility (Dawson, 1993). Because of these special conditions produced it is decided to aim for an engineering alloy.

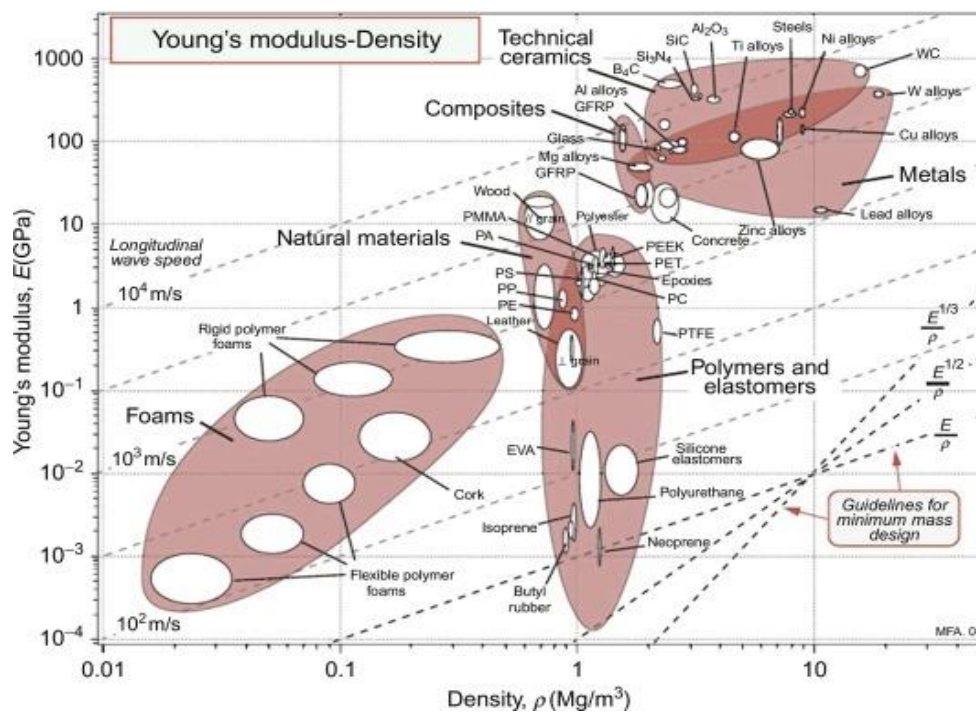


Figure 4 Young's modulus plotted against density for various engineered materials (AL-Oqla & Salit, 2017)

Due to the properties as low density and high strength-to-weight ratios as it can be seen in Figure 4, it is decided to use a light alloy, usually characterized by low toxicity (without including beryllium). Aluminum alloys together with titanium, magnesium and beryllium constitute the group Light Alloys. (Engineering 360, 2015)

From this group of light alloys, it was decided to aim for an aluminum alloy due to economic and density reasons.

## 2.3 Aluminum designation and characteristics

The main advantage of using aluminum in structural applications is having a high strength per density value. This gets more noticeable when compared to other materials such as iron or steel. This condition and its reduced price (due to its abundance in their mineral form), has made aluminum a major choice for transportation. Other interesting characteristics of aluminum are the high corrosion resistance or the high thermal and electrical conductivity. (Royal Society of Chemistry, 2022)

When we focus on casting, these metal alloys have the advantage of having a relatively low melting temperature when compared with other metals as before. Another advantage is their lower solubility to different gases, except hydrogen. This usually brings a good surface finish and fluidity.

The main problem of this metal, coming from one of its main advantages which is the thermal conductivity, is the high degree of shrinkage during solidification that it has. This is a factor that needs to be taken into account during the design step of the process to avoid problems such as bad dimensioning, possible defects or residual stress.

	Current designation	Former designation
Aluminum, 99.00% or greater	1xx.x	
Aluminum alloys grouped by major alloying elements:		
Copper	2xx.x	1xx
Silicon with added copper and/or magnesium	3xx.x	3xx
Silicon	4xx.x	1 to 99
Magnesium	5xx.x	2xx
Zinc	7xx.x	6xx
Tin	8xx.x	7xx
Other element	9xx.x	7xx
Unused series	6xx.x	

Table 2 Aluminum designation (ESAB knowledge centre, 2022)

Cast aluminum alloys have designations to identify as well as group them based on alloy constituents as it can be seen in Table 2. One such designation is the one developed by Aluminum Association of the United States(ESAB Knowledge center, 2022), which uses a four-digit

system and as shown in Table 2.

Regarding the heat treatment, only the 2xx, 3xx, 4xx and 7xx show mechanical improvements after the heating and cooling of the alloy due to the ability to form second-phase precipitates that improve its strength. The other designated alloys can be strain hardened in case it is required although it is not generally applied to castings.

## 2.4 Process selection

Product manufacturing is usually divided in three stages, composed by shaping, joining and finishing. A selection of process affects the shape, the choice of material, and the mass of the product as well as the dimensional precision and surface finish requirements.

At the end of the day, the choice of the process should be cost/quality conscious. In this case, a comparison between a casting process and a pure CNC machining one can be found.

## Theoretical background

On one hand, casting metals is one of the oldest methods of shaping a product. It involves the melting of metals by superheating them, followed by pouring of the liquid metal into a pre-prepared mold, where it is allowed to solidify and take the form of the cavity. Generally, any metal that can be melted can be cast, including the ones that are hard to machine with the other methodology. Its main competitive advantage is the ability to form complex geometries with features like internal cavities, holes or surfaces. Its major disadvantage is the common defects that can entail, including shrinkage and undesired porosities.

On the other hand, the CNC (computer numerical control) machining process (Thomas Company, 2022) is based on the subtraction on material, typically employing computerized controls and machine tools to remove layers of material from a stock piece, producing with it the designed part. This process is suitable

for different materials such as metals, plastics, wood or others. One of its main advantages is the higher achievable tolerances.

These techniques do not rule out one another. For example, if we use a shape casting process, where the goal is to achieve a shape as close to the geometry of the final component as possible (Materials Processing, 2016), CNC machining will be required for the fitting of the different roller bearings and axes. In the case of the CNC machining, continuous casting is needed to create the blocks that will be forged and used in the CNC machine as raw material. In this case, we are focusing on the shape forming stage of both.

### **2.4.1. Casting**

The casting process is mostly commonly categorized into two processes, depending on the frequency of use of mold. These are permanent mold casting and expendable mold casting.

Expendable Mold Casting includes processes like, sand casting, shell casting, investment casting (lost-wax casting), lost foam casting, plaster mold casting, ceramic mold casting, etc. Permanent Mold Casting includes (high pressure-, low pressure-, and gravity-) die casting, centrifugal casting and special processes like rheocasting and squeeze casting.

Due to the low number of copies required in this project, the expendable mold process is further explored.

#### **Expendable mold processes**

There are basically 5 different types of casting processes that require expendable molds such as:

- Sand based modelling
- Plaster mold casting
- Ceramic mold casting
- Investment casting
- Lost-foam casting

## Theoretical background

The first process is the casting with sand-based modelling. This process can be done using four different types of sands that bring different procedures such as:

**1. Green-sand molding:** This type of mold uses non-cured sand as the main element (called green sand) and is the most widely used process. This sand is blended with clay water and additives, leading to a low tooling cost. This system can be applied by drying the whole mold (dry-sand mold) or the part contacting the model (skin-dried mold). This process can have problems with moisture.

**2. No-bake molding:** It is a sand molding process where synthetic liquid resin (organic and inorganic) is mixed with the sand, creating a chemical reaction that hardens at room temperature.

**3. Sodium silicate-CO<sub>2</sub> molding:** This process uses pure dry silica sand (less than 3% moisture) with addition of 3% to 6% sodium silicate. The mold gains its strength from the silicate that quick hardens when exposed to CO<sub>2</sub>. It is usually used when better accuracy, thinner sections, or deeper draws are required than usually achieved by ordinary sand molding. This process cannot reclaim the sand used.

**4. Shell molding:** This process uses a thermosetting resin covered in sand to form a mold. The mixture is dropped, blown or shot onto a heated metallic pattern. This heat cures a layer with the form of the pattern, forming a shell. This shell is usually supported by more sand in a box to withstand the produced stresses. The main advantages of this process are the dimensional accuracy achieved.

The second casting process explained is the plaster mold casting where the mold is made of Paris plaster, a quick setting plaster that hardens after being moisturized, combined with additives to improve its properties. This process gives good surface finished and dimensional accuracy. This plaster has low thermal conductivity and specific heat, which means that the cooling of the casting is really slow, improving its viscosity to fill thin sections and fine details. It is usually limited to metals with low melting points.

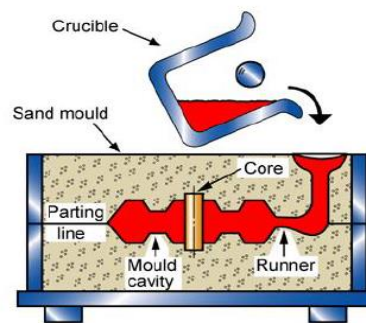


Figure 5 Sand based modeling cast

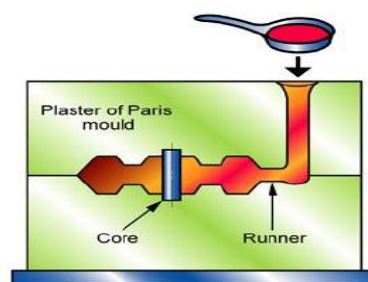


Figure 6 Plaster mold casting



## Theoretical background

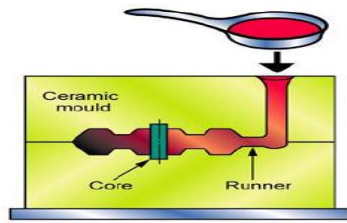


Figure 7 Ceramic mold casting

The third casting discussed is the ceramic mold casting, where the mold is made of ceramic material. This process is able to give fine details, smooth surface and thin sections. These molds have to be preheated before using to ensure the proper filling. It is able to hold metals with higher melting points but it is expensive to produce and the ceramic cannot be recycled.

The fourth process explained is the investment casting, also known as the Lost-Wax casting process. The mold material used in this process is similar as the ceramic mold casting but in this case, the pattern used is disposable because it is usually manufactured using wax. The pattern is not removed prior to pouring the molten metal. When the metal is poured, it melts the wax and vents it out, as it is displaced by the cast metal. Usually, the ceramic shell molds, are making a single patter arranged in a tree-like structure, sharing the gating system.

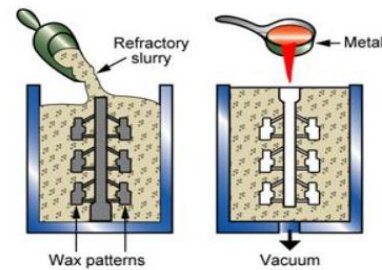


Figure 8 Lost-wax casting

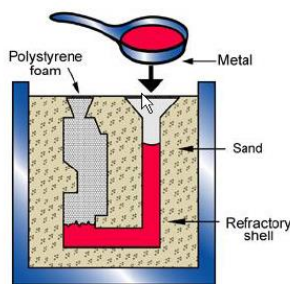


Figure 9 Lost-foam casting

Last but not least, the lost-foam casting, another cavity-less casting process, is similar to investment casting but having sand as a mold material. The patter is made of polystyrene foam. This process needs the use of a flask to get the sand together and it can form different types of patterns. The molten metal is also poured into the pattern, destroying it to create its shape in metal.

From this first research about casting, it can be concluded that the optimal process for the number of pieces required (short badge of 6, 4 to mount on the system and 2 spare) and taking into account the rather lower requirements of surface finish and precision before the CNC machining, the sand-based casting using green sand (Sadayappan & Elsayed, 2018) is the chosen process.

The used model for this procedure will be a 3D printed one to simplify the process and achieve the required shape.



## 2.4.2. CNC machining

Depending on the type of piece to manufacture, there are different types of CNC machines to use. It also depends on the function they perform, the materials that are about to be used and the technology needs for it.

With this classification there are 8 types of CNC (John, 2021) machines that can be seen in Table 3:

<b>CNC type</b>	<b>Function</b>	<b>Materials</b>	<b>Axes</b>
Milling machine	Face milling, turning or shoulder milling	Wide range	3 cartesian 3 rotational
Router machine	Face milling, turning or shoulder milling	Soft materials	3 cartesian
Plasma cutting machines	Cutting	Metals	2 cartesian
Lathe machines	Turning	Wide range	2 cartesian
Laser cutters	Cutting	Wide range	2 cartesian
Water-jet cutter machine	Cutting	Wide range	2 cartesian
Electrical discharge machine (EDM)	Face milling, turning or shoulder milling	Conductive	3 cartesian
Grinder machine	Face milling, turning or shoulder milling	Wide range	3 cartesian 3 rotational

*Table 3 Types of CNC machines (John, 2021)*

From this research about the types of CNC machines, it can be concluded that the optimal machine would be a milling machine with some modifications to simplify the optimized shape.

### 3 Problem description

During this chapter, the design process followed for the robot is going to be explained, including the requirements, the calculations and commercial pieces used, and a first draft will be shown.

#### 3.1. Concept design

In order to integrate the three different types of wheels it was decided to place them all in each of the four axes. The different types of displacement modes, prioritize different characteristics such as:

- Rubber wheel position – The velocity is prioritized; the traction of the system will increase.
- Mecanum-wheel position – The maneuverability is prioritized and allows the CERNBot to move in all directions.
- Track position – The traction with steep angles is prioritized, allowing the robot to go upstairs.

Considering the dimensions of the different items that need to be placed and so they don't interfere with each other during the displacement or the traction system change, the working positions were defined as can be seen in Table 4.


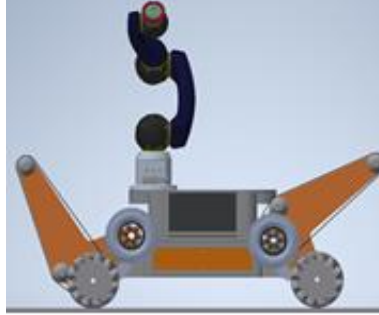
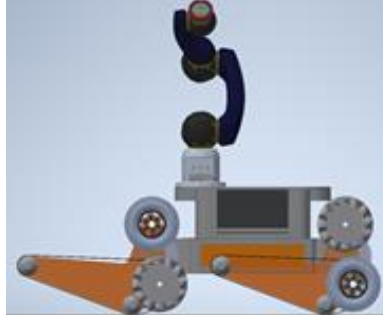
Rubber wheel position	Mecanum-wheel position	Track position
		

Table 4 Required positions of the CERNBot

##### 3.1.1. Technical requirements

One of the requirements established by the operational team of the robot is that it should be capable of doing a whole lap on the LHC in less than 3 hours (27 km). Another requirement is that the robot should be able to change autonomously from one wheel system to another in 10 minutes or less.

Taking that into account, the requirements are:

- Required velocity – 10 km/h
- Required turn velocity – 5 rpm

## Problem description

- Required step angle –  $45^\circ$
- High of the step – 200 mm

### 3.2. Forces applied

#### - Static forces

The first needed calculations are the motor-reduction requirements to be able to climb the stairs. In order to do so, it is taken the first concept design and the reaction forces are calculated.

In order to simplify the control of the system, it is decided that the back turning system is going to be fixed in a specific angle. This situation gave us the variables that can be seen in Figure 10.

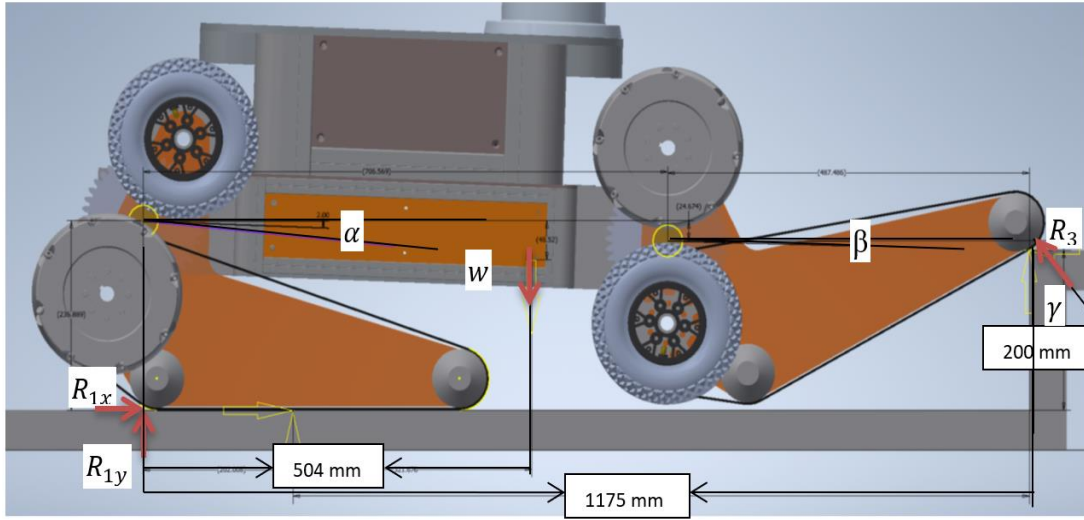


Figure 10 Forces and angles in the CERNBot stairs positions

Where the angles will work as follows:

- $\alpha$  will be the inclination angle between the horizontal axis and the main body part from the back rotation axis.
- $\beta$  will be the angle between horizontal axis and the contact point with the stairs from the front rotation axis.
- $\gamma$  will be the angle between the vertical axis and the normal reaction from the robot.

With those variables we developed the following equations:

$$\sum F_x \rightarrow -R_3 \cdot \sin(\gamma) + R_{1x} = 0$$

$$\sum F_y \rightarrow -w + R_3 \cdot \cos(\gamma) + R_{1y} = 0$$

$$\sum M_1 \rightarrow -w \cdot 0.504 + R_3 \cdot \cos(\gamma) \cdot 1.175 + R_3 \cdot \sin(\gamma) \cdot 0.2 = 0$$

## Problem description

Where the assumed weight of the system including the traction is approximately 190 kg, giving a value of 932 N (assuming a gravity of 9.81 m/s<sup>2</sup>) per wheel. This situation leaves a value of  $W$  of 466 N because there will be both sides on contact with the floor.

To determine the worst-case scenario, where the reaction forces would be the highest, it was decided to fix the furthest point of the track system on the tip of the stair and do a sweep of values of  $\alpha$  from  $-2^\circ$  to  $2^\circ$  in intervals of  $0.1^\circ$ . This method established the worst-case scenario when  $\alpha$  has a value of  $2^\circ$  and, consequently,  $\beta$  is  $1,4^\circ$  and  $\gamma$  is  $27,6^\circ$ .

This scenario gives a value for the reactions as seen below.

$R_{3x}$	$R_{3y}$	$R_{1x}$	$R_{1y}$
192 [N]	367 [N]	192 [N]	565 [N]

From these reactions, we isolate the traction system to achieve the required torque from the motors. Isolating the front uphill system, we take the distances and forces from the turning point, as it can be seen in figure 11.

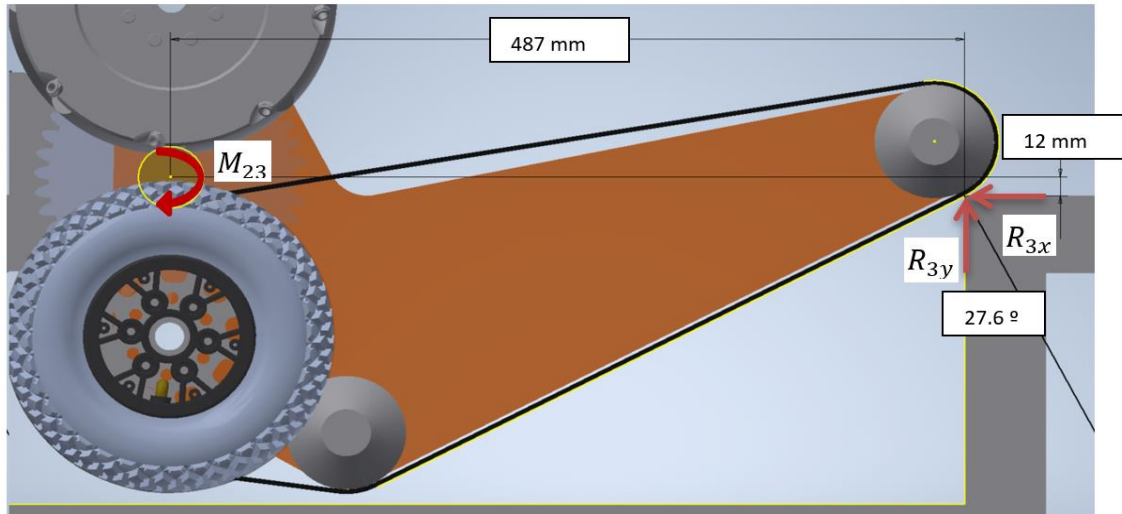


Figure 11 Front wheel track in the CERNBot position

Following those variables, we developed the following equations:

$$\begin{aligned}\sum F_x &\rightarrow R_{3x} - R_{23x} = 0 \\ \sum F_y &\rightarrow R_{3y} - R_{23y} = 0 \\ \sum M_1 &\rightarrow R_{3y} \cdot 0,487 + R_{3x} \cdot 0,012 - M_{23} = 0\end{aligned}$$

These equations gave the following forces and torque:

$R_{3x}$	$R_{23y}$	$M_{23}$
192 [N]	367 [N]	181 [Nm]

## Problem description

### - Traction forces

Another required calculation is the combination motor-reduction for the traction. In order to do so, the first concept design is used to calculate the reaction forces and the minimum force required. It is assumed that track will be flat in order to increase the traction.

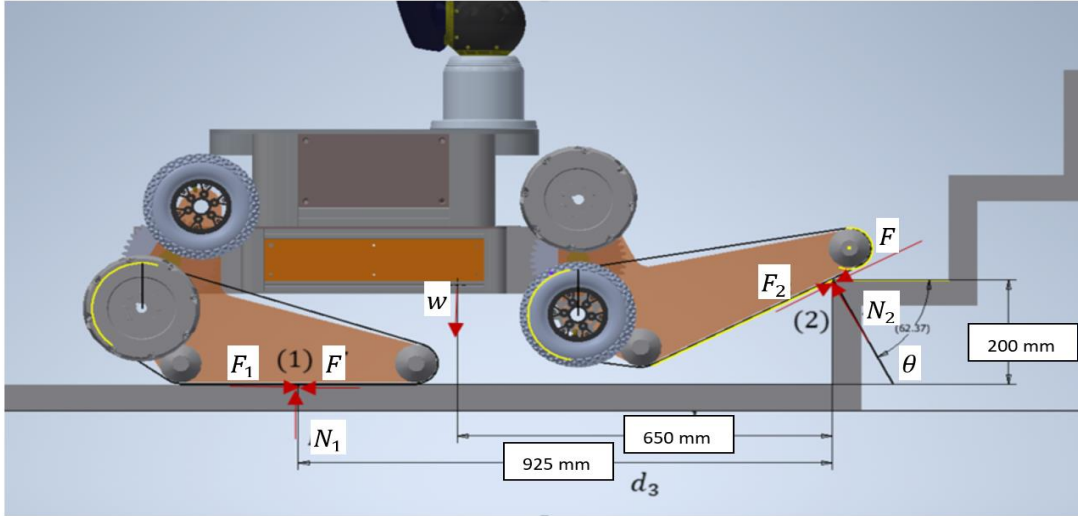


Figure 12 Required torque calculations and variables

Where the angles will work as follows:

- $\theta$  will be the angle between the vertical axis and the normal reaction from the robot.

Following those variables, we developed the following equations:

$$\sum F_x \rightarrow -F - F \cdot \sin(\theta) + \mu_c \cdot N_1 + \mu_c \cdot N_2 \cdot \sin(\theta) - N_2 \cdot \cos(\theta) = 0$$

$$\sum F_y \rightarrow -w + N_1 + \mu_c \cdot N_2 \cdot \cos(\theta) + N_2 \cdot \sin(\theta) - F \cdot \cos(\theta) = 0$$

$$\sum M_2 \rightarrow F_1 \cdot 0,2 - N_1 \cdot 0,925 - F \cdot 0,2 + w \cdot 0,650 = 0$$

A value of  $\mu_c$  of 0,37 is assumed. After another angle sweep of  $\theta$  using intervals of  $0.1^\circ$  with values from  $45^\circ$  to  $62,4^\circ$  (which is the maximum reachable angle without changing the rear axis angle), it is seen that the worst-case scenario for the traction happens when  $\theta$  has a value of  $62.4^\circ$ . This scenario gives a value for the reactions as seen below.

F	N1	N2
128 [N]	741 [N]	237 [N]

The maximum required torque will be the one applied on the pneumatic wheel, taking into account that it is the biggest one. The selected pneumatic wheel has a radius of 0.04 m, and consequently, the minimum required torque is 5,1 Nm.

Considering that the wheel change will bring an acceleration of the whole system, this acceleration will add more force to the already calculated reactions. The force is considered negligible assuming a low wheel change velocity.

### 3.3. Industrial components

After a comparison with different manufacturers and industrial companies, it is decided to aim for the following motors and reductions:

#### Traction system components



Figure 13 Traction motor chosen

##### Motor Nanotec DB80 (NANOTEC SL, n.d.)

BLDC motor 8 poles and very high-power density. With a rated voltage of 48 V, particularly suited for applications requiring high efficiency.

Model: DB80C048030-ENM05J

Torque	Velocity	Power
3 Nm	3000 rpm	942 W

#### Wheel change system components



Figure 14 Stepper motor selected for the wheel change

##### Motor Anaheim 42Y (Anaheim Automation, 2015)

Stepper motor with high torque, designed to minimize the vibration and audible noise. Standard 8-lead motors. 1.8° step angle

Model: 42Y312S-LW8

Torque	Velocity	Power
10 Nm	300 rpm	400 W

##### Single axis slew drive KMI Kinematics (Solar Drives, n.d.)

HE slew drive with multiple mounting and torque tube configurations.

Model: KMI Kinematics HE3

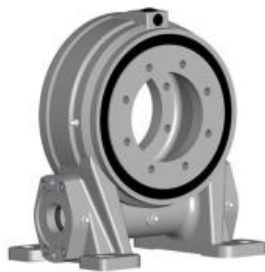


Figure 15 Reduction selected for the wheel change

Torque	Velocity	Efficiency
620 Nm	5 rpm	0.7

### Characteristics

Using the elements shown before, the characteristics that this equipment will develop are:

- Total weight – 25kg

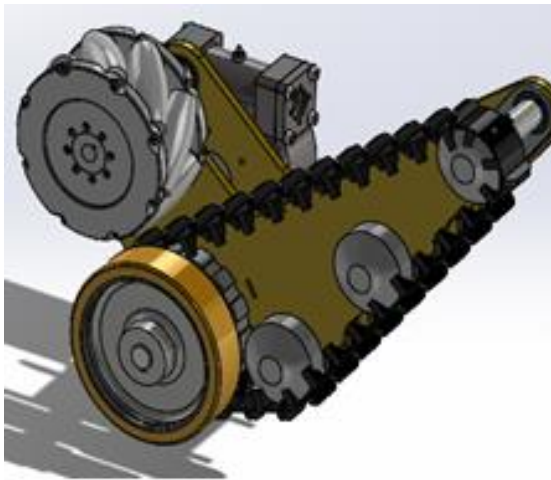


## Problem description

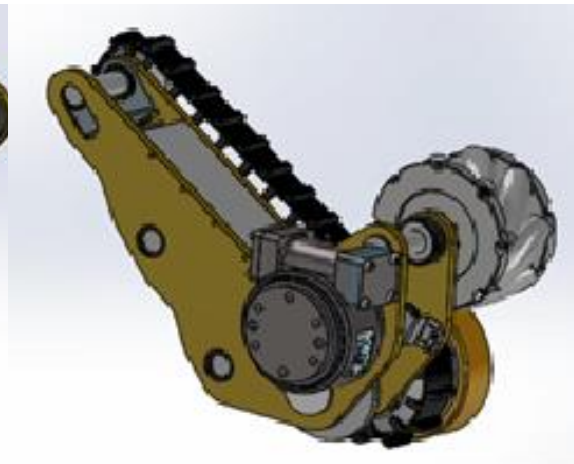
- Max. traction velocity – 600 rpm
- Max. traction torque– 15 Nm
- Max. turn velocity – 5 rpm
- Max. turn torque – 620 Nm
- Max. step angle – 45°
- Total payload with the designed system after removing the weight of the previous traction system- 190 kg

### 3.4. Concept draft

After evaluating the fitting of the components mentioned on the previous chapter and including roller bearings, shafts and the three types of traction, the final disposition of the elements can be seen on Figure 16 and 17.



*Figure 16 Conceptual draft front*



*Figure 17 Conceptual draft back*

All this system will be held using the 6xM6 screws connected to the reduction system from KMI Kinematics that will be installed on the body of the CERNBot. The Nanotec motor is mounted using 4 M4 screws into a build-in plate in the structure of the system as it can be seen on Figure 13, along with the tensioning mechanisms for the power transmission belt and the track system.

The pneumatic wheel and the track are activated by the same shaft, connected by a key to transmit the torque as it can be seen in Figure 20.

The reinforcement plate placed at the top of the system can also be seen, covering the electric motor and gears and improving the structure stiffness.

## Problem description

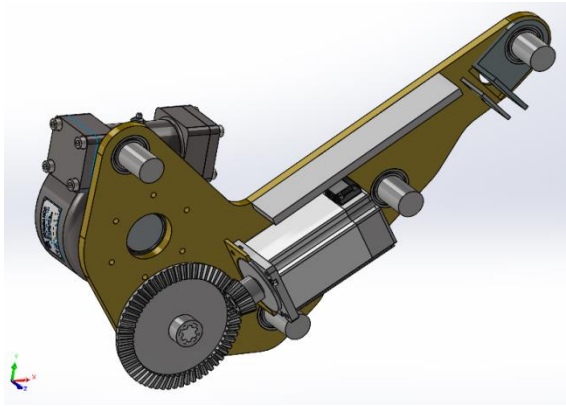


Figure 18 Traction motor connection with main shaft

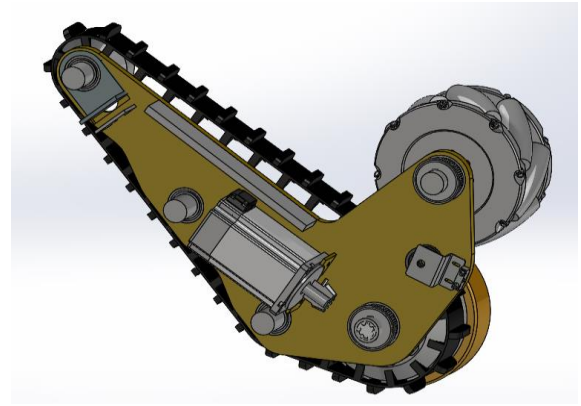


Figure 19 Pulley gears for the traction transmission

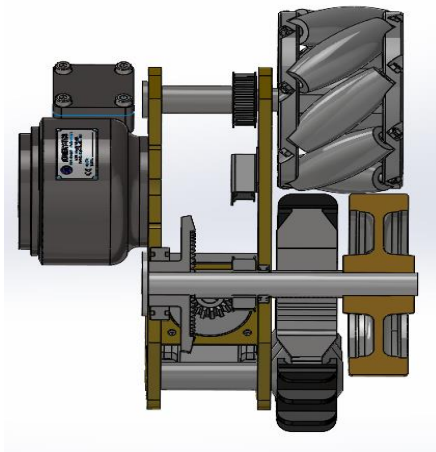


Figure 20 Main shaft of the transmission system

This concept relies on one motor, used for the turning of the three types of wheels.

First, the Nanotec motor is connected to a conic gear with a relation of 1:5 in order to increase the torque and reach the required 15 Nm. This conic gear is mounted at 90 degrees, transmitting the power to the main shaft via a keyhole. This same shaft has connected the pneumatic wheel and the drive wheel for the track, using the same method.

At the same time, the gear for the pulley is connected using a belt (with a relation 1:1) that will transmit the power to the upper shaft which is in charge of moving the mecanum-wheel. All this system can be seen on Figure 20.



## 4 Simulations

In order to improve the designed piece and ensure the behavior of the system, a FEM simulation was done.

### 4.1. Introduction to FEM analysis

The Finite element method (FEM) is a mathematical method to solve partial differential equations where the mathematical model that we need to solve is divided into simple geometrical objects called finite elements.

The response of each finite element is described by a polynomial, leading to a finite number of degrees of freedom (DOF's). The response of the system is obtained when we combine all the responses of the different elements. These elements can be chosen depending on the shape that we are willing to analyze and the accuracy and dimension that this will have. This division of the component is called mesh, and it needs to be adapted to the requirements and expected forces.

The division and focusing in different parts become more important when we are simulating casting. This happens due to the change of properties that the different solidification can bring to the used material. In the regular FEM analysis, a homogenous definition of the material properties is used that we will later use to solve the DOF's.

In this thesis, the main objective of the use of FEM is to achieve a lightweight piece, with an acceptable deformation and capable of holding the stresses that it will receive.

### 4.2. Mechanical simulations

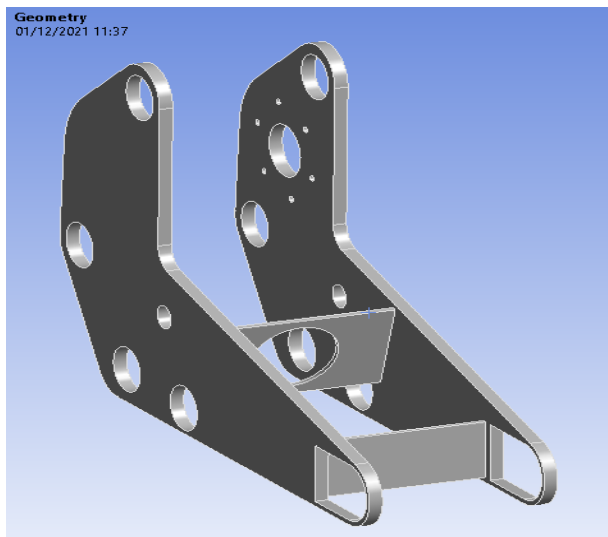


Figure 21 Basic structure simulated and optimized

The program selected to simulate the behavior of the design is ANSYS 19.1

The component that is simulated is the whole structure that will hold the system together, including the industrial components mentioned before. This piece weights 5.4 kg

In each of these simulations, we are going to aim for the stress and deformation occurred in the 4 system positions that compose the solution to simplify the required calculations.

The 4 simulated positions are:

- Track before upstairs position – Position prior to the climbing of the stairs. This position is assumed to be one of the worst case scenarios, where most stress Will be applied to the structure.

## Simulations

- Pneumatic wheels - Position of the structure where pneumatic wheels are used
- Mecanum-wheels – Position of the structure where mecanum-wheels are used
- Track on the stairs position – Position of the wheels where the track is being used.

The material used after several simulations where the selected aluminum (6000 series, 4000 series...) was an overkill is an Aluminum 2000 due to the low requirements. This condition will be stated in the following simulations. Specifically, the Aluminum used is the 2024-T4 (*ASM Material Data Sheet*, 2001) with the following properties:

Density	Hardness, Brinell	Tensile strength	Yield strength
2.78 g/cc	120	469 MPa	324 MPa

An equivalent that will be used later on in the casting simulation is the AlCu4Mg1 (*Aluminium-Copper Alloy (ISO AlCu4Mg1)*, n.d.) with the following composition.

Element	Aluminum 2024-T4	AlCu4
Aluminum	90.7-94.7 %	93.2%
Copper	3.8-4.9 %	4.5 %
Magnesium	1.2-1.8 %	1.5 %
Manganese	0.3-0.9 %	0.6 %

Table 5 Composition of the used aluminums

After these simulations, a topological optimization will be applied on the different positions to observe the sections of the structure where material can be reduced. Considering that all forces are opposed, the fact of using a combination of the forces for all position would result in the cancelation of the different forces and, consequently, a smaller expected force than the real one. Afterwards they will be combined into one piece by using as a reference the attachment points and the traction axes. After this combination, the piece is compared with the original and the parts where material it can be reduced can be seen.

### 4.2.1. Mesh quality

One of the most important parts of a simulation is to achieve a proper quality of mesh. In this case, a hexagonal mesh of elements of first order with a size of 0.5

## Simulations

mm has been used due to its good quality in straight surfaces. To improve its quality in complicated areas, the mesh has been personalized around the axes that will receive load.

Some modifications have been applied into the piece to simplify the calculations, such as a thin cylinder to simulate the connection that will be made using the axis, or the simplification of some roller bearing housing shapes, due to the problematic to achieve a good mesh quality (Ferris, 2020).

Most of the piece achieved a quality mesh of 0.75 as minimum, but some parts (mostly around the connections for the axes), suffered a decrease of the quality due to its round shape.

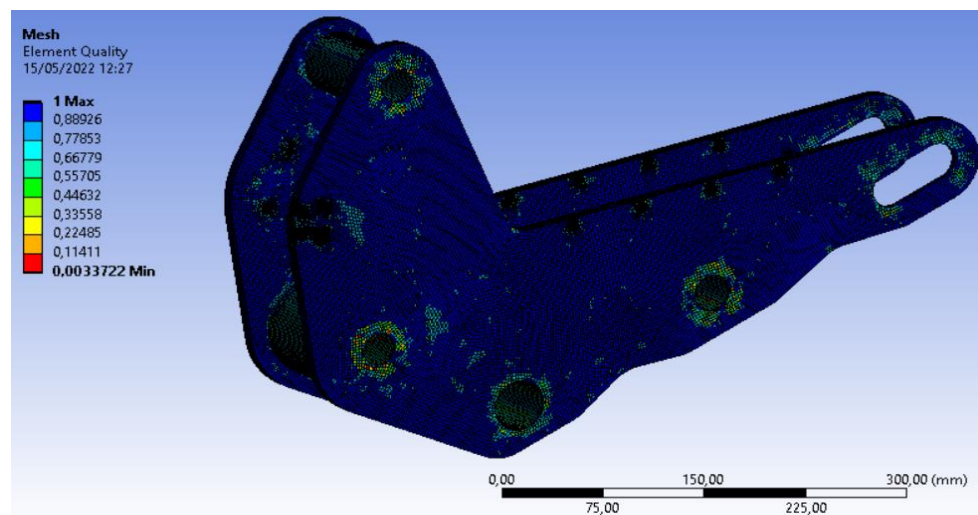


Figure 22 Mesh quality values for the FEM simulations in ANSYS 19.1

### 4.2.2. Simulation results

The general boundary conditions applied to these simulations are as follows:

- Fix the side displacement on the face attached to the robot.
- Fix the axis that will be in contact with the floor during the simulated position.
- The weight of the robot of 932 N in order to leave a safety factor of 1.2 considering a total payload of 620 N (64 kg) or 310 N per side. This weight is applied in the holes made for the gear reduction attached and the direction is adapted depending on the traction requirements.
- The preload applied for the track to keep the tension of 150 N in the plate that will hold the tension system
- Traction motor weight of 35 N in the plate that will house the motor.

The maximum values achieved by the stress and deformation simulations can be seen in Table 6.

Simulations

	Track before upstairs	Pneumatic wheels	Mecanum-wheels	Track on the stairs position
Max deformation	0.01 mm	0.001 mm	0.04 mm	0.24 mm
Von Mises stress	7.4 MPa	7 MPa	7.4 MPa	27.6 MPa

Table 6 Ansys 19.1 stress and deformation simulation results

As expected, the deformations that this structure will receive and considering the applications that it will need, can be neglected.

Further information and images regarding the simulations and boundary conditions be found in Appendix 1.

- Topology optimization

In the case of the boundary conditions for the topology optimization, a 60% mass reduction is applied, leaving the attachment and housings of the structure out of the scope of this reduction. These optimizations show the results of Table 7.

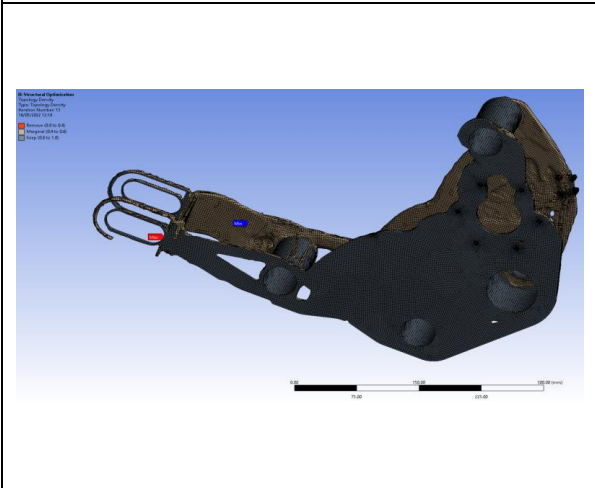
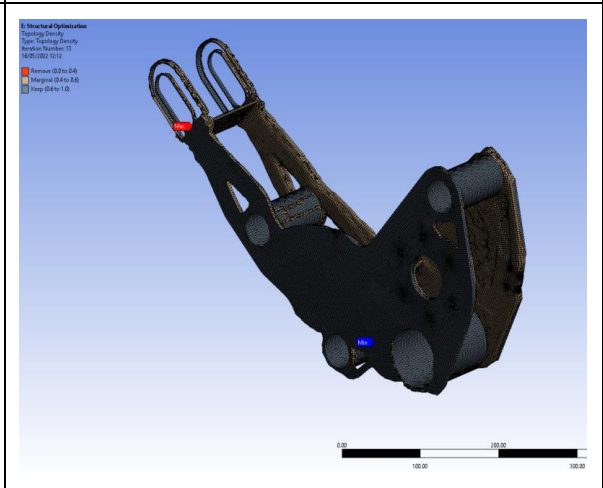
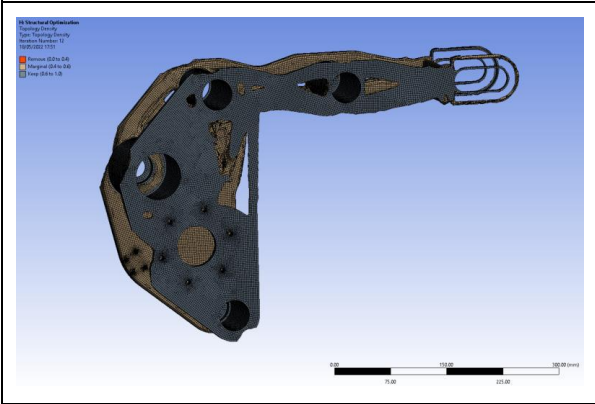
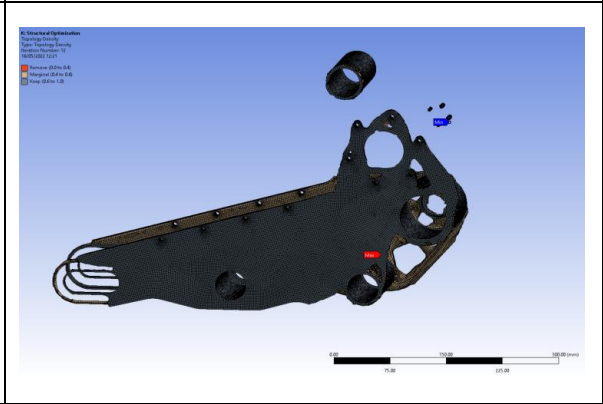
Track before upstairs	Pneumatic wheels
	
Mecanum-wheels	Track on the stairs position
	

Table 7 Ansys 19.1 structure topology optimization results

## Simulations

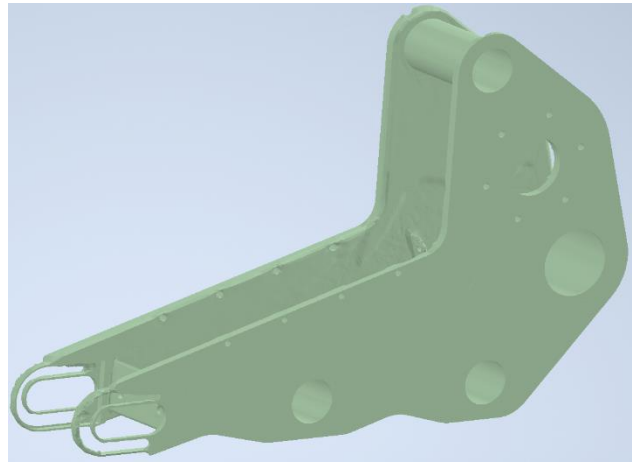
As it can be seen, these optimizations cannot be applied directly into production, but they give a guideline of the places where an excessive amount of material have been used.

### Optimized model

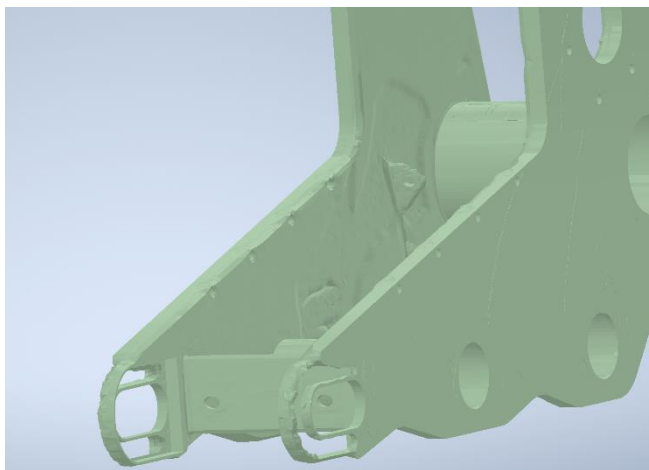
As stated before, it is proceeded to combine the figures of Table 7 to consider the different requirements that those positions had.

As it can be seen, the piece remained similar in shape due to the different forces that it will be receiving from different angles.

Most of the reduction happened on the outer side of the structure, where the thickness of the plate has been reduced by 3 mm in some spots such as the one that can be seen in Figure 24.



*Figure 23 Exterior of the fully optimized piece*



*Figure 24 Internal view of the fully optimized piece*

Another component that got reduced is the connection for the traction system that is used as a guide and is not receiving force.

Last but not least, the plate to connect the motor got reduced into 4 brackets.

The combination of the different optimizations and considering some restrictions such as roller bearing housings or other position requirements left a mass saving of around 25%, leaving it at about 4 kg.

### 4.3. Final models

In this subsection we will observe the two different designs that the optimized model gave, considering the different requirements that the manufacturing using machining and the manufacturing using casting have.

#### Cast model

The original piece was adapted following the guidelines of the topology optimized piece. In this case, the external plate got reduced by 3 mm and the support for the tensioning system got emptied, leaving the minimum material needed to hold it in position. All these modifications left a weight of 4.2 kg.

## Simulations

After this piece is cast, it will need to go through a CNC machine to smooth the surfaces for the housings of the roller bearings and ensure the smoothness of the surface for the tensioning system.

Due to this requirement, the piece got divided in two castable pieces and the thickness of the tension plate got increased by 5mm to reduce the deformation.

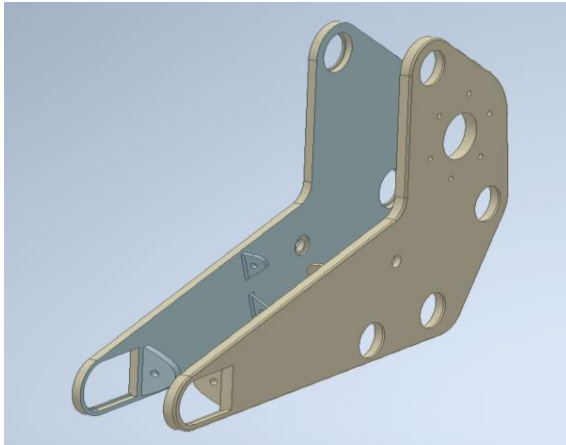


Figure 25 Front view of the cast piece after being machined

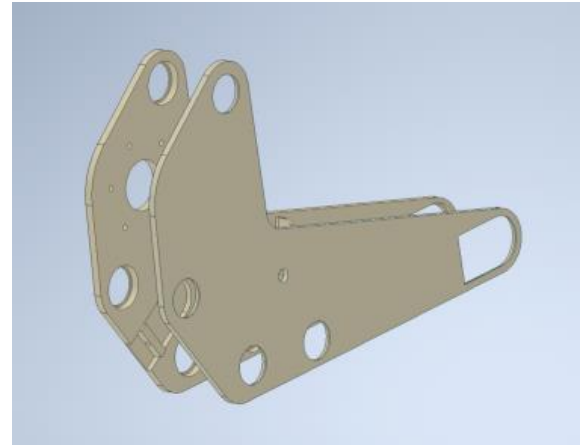


Figure 26 Side view of the pieces after being machined

## Machining model

Due to the complexity of the piece, it is not possible to manufacture this structure in one piece using CNC machining, so it is decided to divide it into 4 different pieces that will be welded after production.

Those pieces will be both sides of the model, the tension plate for the track system and the attachment for the motor. Those two last pieces can be manufactured using a CNC laser cut machine in a 4 mm Aluminum sheet to reduce the price.

The pieces that will need to be manufactured using a CNC milling machine have been adapted to reduce its complexity into easier shapes, in sacrifice of performance and weight. Following the indications of the topology optimization, the exterior side plate width has been reduced 3 mm, leaving a weight of 4.2 kg.

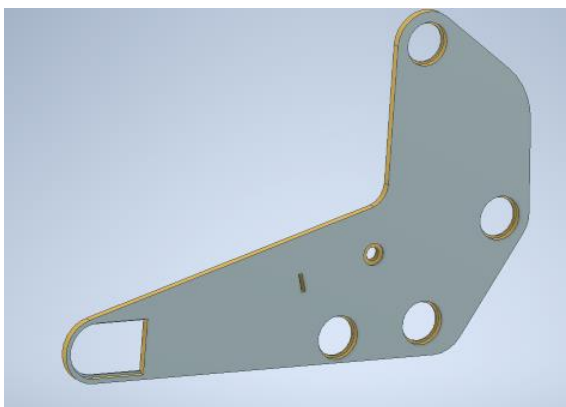


Figure 27 External side bracket of the structure

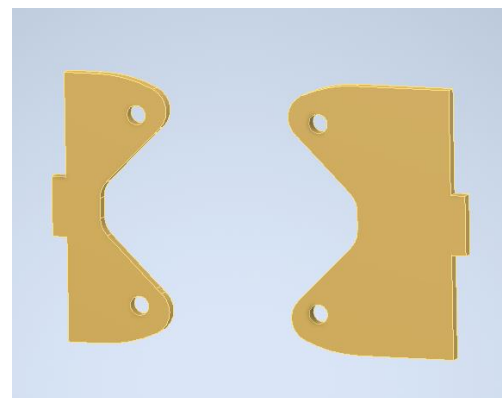


Figure 28 Motor attachments



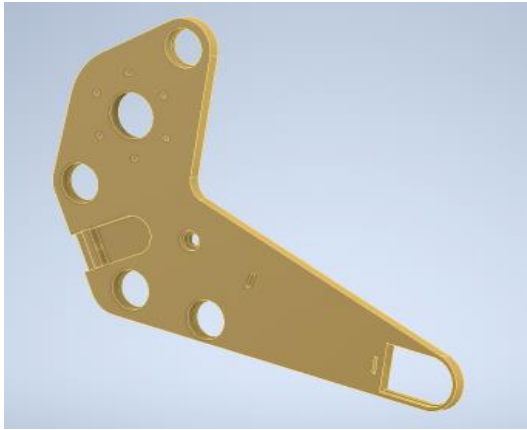


Figure 29 Internal side bracket of the structure

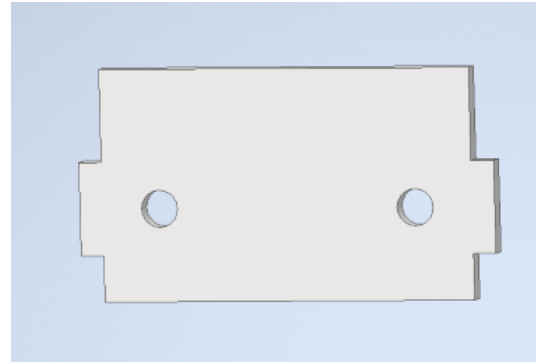


Figure 30 Track tension plate of the structure

## 4.4. Casting simulation

### 4.4.1. Cast geometry

#### 4.4.1.1. Piece modifications

The original geometry of the chassis was believed to be too complex in some spaces due to the following features:

- Small sized threaded holes, lateral and vertical, with a smooth finish or threaded
- Undercuts with smooth finish applied to allow tensioning systems to be housed.
- Surface roughness of Ra 1.6 (SKF, n.d.) for the housings of the roller bearings.

All the features explained above will be done in the after-processing with a CNC machine.

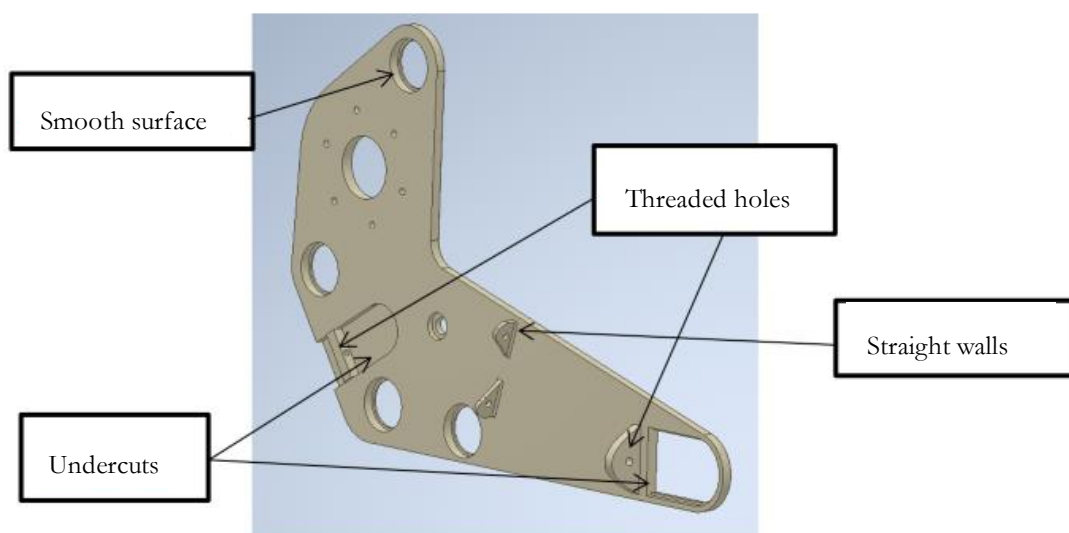


Figure 31 Geometry required modifications

## Simulations

The features discussed above were difficulties for casting these pieces and were minimized by modifying the geometry (Gwyn, 2008) as it can be seen in figures 32 and 33.

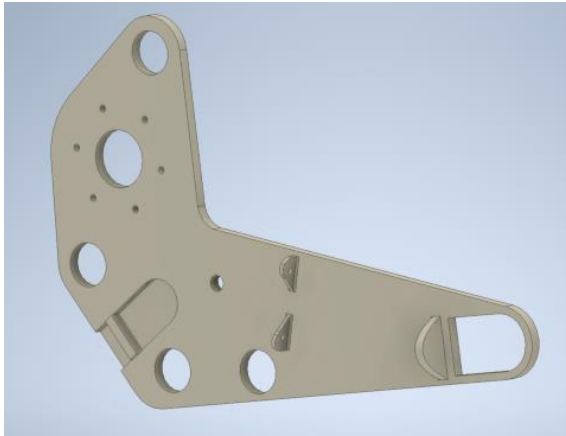


Figure 32 Final interior support to be cast

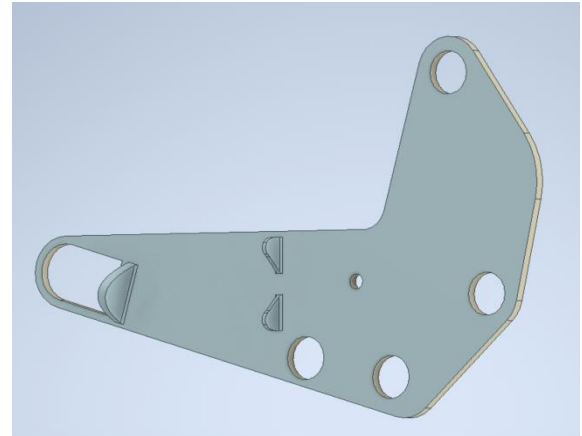


Figure 33 Final exterior support to be cast

Some rounding's have been also included in the brackets for the motor and the tension system to avoid sharp corners when possible

Moreover, some of the casting processes require specific draft angles, fillet radii or minimum wall thickness that should be taken into consideration while modifying the structure. In this case, draft angles of  $2^\circ$  were included following the extraction faces as seen in Figure 34. The fillet radii can be corrected in case of need with the CNC machining. All the piece has a minimum thickness in all its parts of 4mm, produced in the undercut for the tensioning system.

For these two pieces, the casting position will be as follows in order to reduce the size of the box needed and making both pieces lie flat:

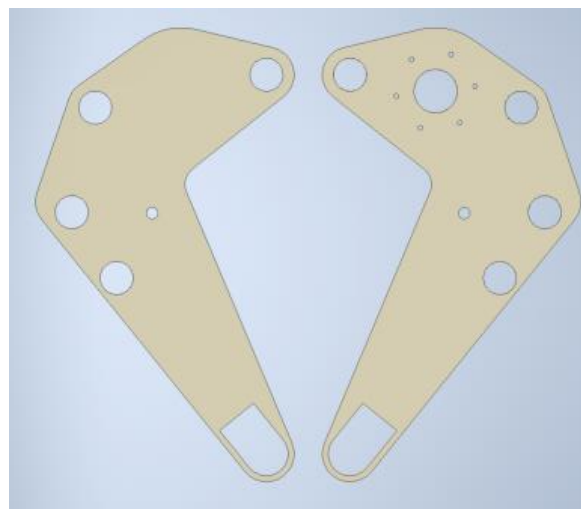


Figure 34 Cast pieces mold disposition

### 4.4.1.1. Gating system

In order to simulate the casting process on the new geometry, the gating system had to be first designed.



## Simulations

The main components to study on the gating system are:

- Pouring cup
- Sprue
- Well
- Runner
- In gates

In this case, it is going to be assumed that the melt it is going to be poured from a hand-held ladle.

We will be using a normalized conical pouring cup with an upper diameter of 70 mm and a high of 152 mm. This piece is needed due to the reduction of turbulence and vertexing it brings and also because it helps separating dross, slag and foreign elements.

To calculate the dimensions of the down sprue we will use the equations of a free-falling stream (from zero, taking into account that this process will be gravity driven) and the conservation of matter. Thus, the velocity of the melt in free falling conditions:

$$v = \sqrt{2gh}$$

And from the conservation of matter from the top and the lower sections of the sprue:

$$Q = v_1 A_1 = V_2 A_2$$

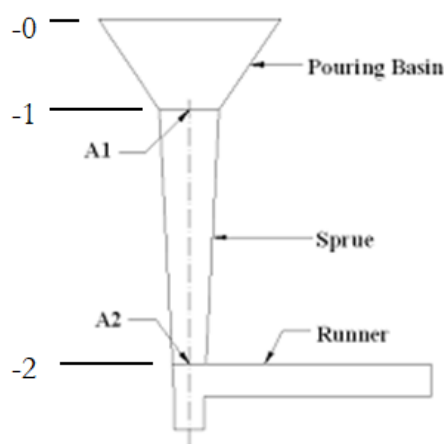


Figure 35 Sample sprue and pouring basin

The relation equations are at the two heights of the sprue as seen in Figure 64. Thus, those two equations will give values at the entrance and exit of the sprue.

Assuming that pouring from the ladle starts at the top of the pouring cup, (H-0), the melt drops at a height of 152 mm to get to the top of the sprue.

The top of the sprue (H-1) should be placed higher than the maximum reachable point to the cast part, related to the piece placed. This distance is 45 mm and we will add 20mm to increase the pressure of the melt and help it reach more complicated areas.

This equals to a drop of 215 mm in the sprue which, applied to the velocity equations gives the following results:

Velocity 1	$v_1 = \sqrt{2 \cdot 9.81 \cdot 0.152}$	1.72 m/s
Velocity 2	$v_2 = \sqrt{2 \cdot 9.81 \cdot 0.217}$	2.02 m/s

## Simulations

A point to consider would be that the maximum theoretical speed that the melt should reach is 0.5 m/s to avoid turbulent flow on the melted metal. Since with such large surface this speed was difficult to avoid, it is decided to try to contain the melt to close-bound by the sprue walls that should have a hyperbolic shape (Teklu & Marcos, 2009). This is done to avoid splashing. Due to the difficulty of implementing a hyperbolic shape it is decided to use straight walls instead.

As the products mass is 4.2 kg and we are assuming a filling rate of 1 kg/s, we get a filling time of 4.2s which is an acceptable filling time without considering the mass of the ingate system.

To calculate the sprue entrance and exit areas, the volume flow rate has to be calculated as:

$$\dot{Q} = \frac{\dot{m}}{\rho}$$

Where  $\dot{m}$  is the fill rate assumed and  $\rho$  is the density of aluminium at melting point of 680 °C (Abd Razak et al., 2017).

Filling rate	$\dot{Q} = \frac{\dot{m}}{\rho} = \frac{1}{2500}$	$4 \cdot 10^{-4} \frac{kg}{m^3}$
--------------	---	----------------------------------

The use of this filling rate results in the following required areas at the entrance and exit of the sprue. If we consider a conical sprue, we also get the following diameters.

Area 1	$A_1 = \frac{Q}{v_1} = \frac{4 \cdot 10^{-4}}{1.72}$	$A_1 = 232 \text{ mm}^2$	$\varnothing 17.2 \text{ mm}$
Area 2	$A_2 = \frac{Q}{v_2} = \frac{4 \cdot 10^{-4}}{2.02}$	$A_2 = 198 \text{ mm}^2$	$\varnothing 15.8 \text{ mm}$

In this case and due to the higher velocities expected, a well is going to be used to reduce the speed of the melt before entering the runner. This well will have a cross sectional area 5 times the one of the sprues exits, with a depth twice the runners (Hasse, n.d.)

This means that it will have an area of 990 mm<sup>2</sup> and consequently  $\varnothing 35.5 \text{ mm}$ .

The cross-sectional area of the runner extension is set as the same as the outlet of the sprue, converted into a rectangular section with the width of the diameter (15.8 mm) which leaves a depth of 12.5 mm.

In the case of a multiple gating, the tendency of the stream is to flow through the path of least resistance, which means that a large portion of the molten metal will flow through the last gate. As the first law of motion states, the stream of metal tends to continue moving in the same direction until an outside force is exerted to change it. In this case, the outside force will be the reduction of the cross-sectional area of the runner just beyond the first gate in proportion to the number of gates passed.

## Simulations

For that reason, and the reduction of turbulence and slag, it is decided to aim for a stepped runner, with 2 steps.

In the case of the ingates, two of them will be used dividing the runner's area into three different ingates, two directed to the casting and an extension of the runner to hold the slag. This will leave an area of 99 mm<sup>2</sup>.

After a first simulation using MAGMAsoft without any ingate and with the conditions explained on section 4.3.2, we get the porosity observed in Figure 36.

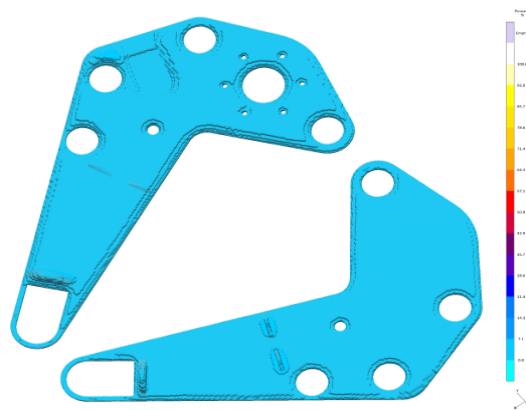


Figure 36 Porosity check for the ingate positioning

A large surface shrinkage can be observed but no big hotspot appears. The lack of a specific hotspot implies that the ingate connection will be focused on the parts where the mass is going to be higher. In this case, they will be installed on the traction motor brackets and on the upper part of the piece to distribute the liquid evenly.

With all the explained above, the gating system would look as follows:

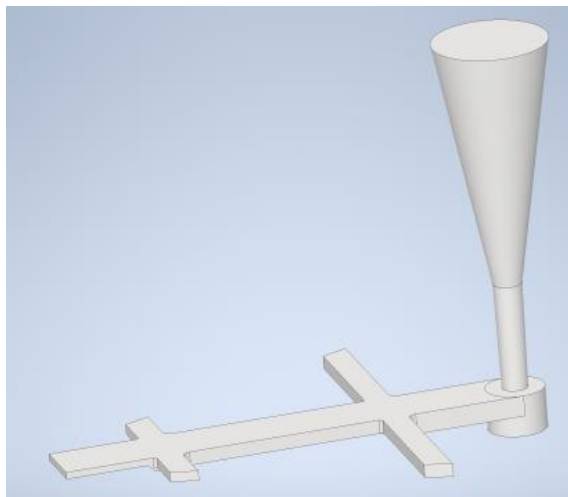


Figure 37 Gating system for the structure

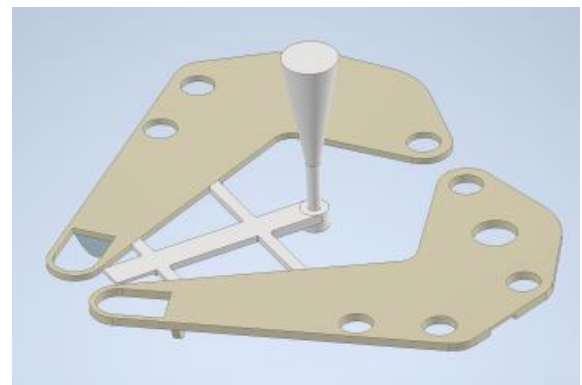


Figure 38 Ingate connection to the brackets of the system

This system will also include risers to ensure the correct filling of the cavity and the reduction of the porosity on the surface.

### 4.4.2. Simulation setup

The gating system along with the whole system were modelled with Inventor and imported in a STL file to MAGMASOFT 5.5.1, which is the program used to simulate the casting behavior.

## Simulations

The meshing of the geometry was done with the automatic mode using finite difference method and hexahedral mesh elements. Considering that the program requires two cells in the thinnest wall of the cast piece, the piece required a total of 3.000.000 cells, and in order to get an accurate representation of all the shapes, paying special attention (considering the hexahedral shape) to the round geometries as seeing in figure 39.

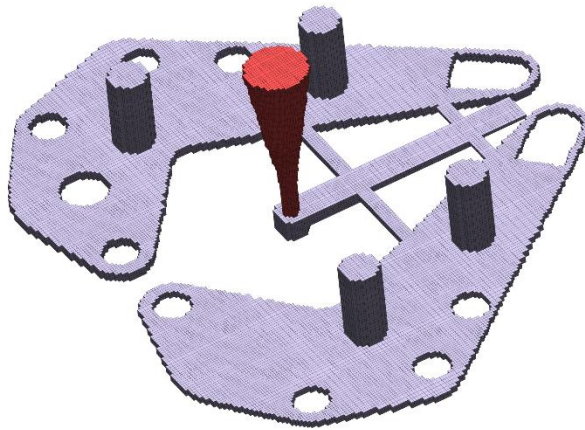


Figure 39 Mesh for the simulation

The main disadvantage when used such small size mesh elements is the increase of computational time.

When discussing about the parameters for the simulation, the first step was the calculation for the filling and the solidification and the selection of the different materials. The ingate, runner, well, sprue and pouring cup, as well as the pieces and the risers used the same material, AlCu4Mg1 as stated before for the stress simulation. For the sand, we used a generic green sand and in the case of the required cores, the furan core was used. All these materials could be found in the MAGMASoft material data base, with the default usages of them.

The initial temperature used for the molten aluminum was 680 °C, while for the mold a preheated value of 200°C. Although this an atypical temperature for green sand casting and it will imply more work, it was chosen in order to keep the temperature over the liquidous line for longer periods of time and prevent the early solidification of the metal (Tasaki et al., 2018). This preheating also helps to reduce the burr thickness produced. In addition, a heat transfer coefficient dependent on the temperature between the sand mold and the casting metal was used. A pouring time calculated before as 4.2 s is also stated.

### 4.4.3. Results

In the next two subsections the filling and the solidification simulation results will be discussed.

#### 4.4.3.1. Filling results

In order to achieve a smooth filling of the cavity, we need to consider the critical velocity of the melt inside during the filling, being it approximately 0.5 m/s. Although this velocity is usually exceeded (it is reached with a drop of 12.5 mm), it is considered the velocity where the filling produces less defects. Thus, if it cannot be helped, the criteria needed is to contain and channel to avoid splashing.

The fact of using multiple gates, implies that the probability of creating hotspots gets reduced, but they might take too short time to solidify and prevent the rest of the melt to enter the mold.

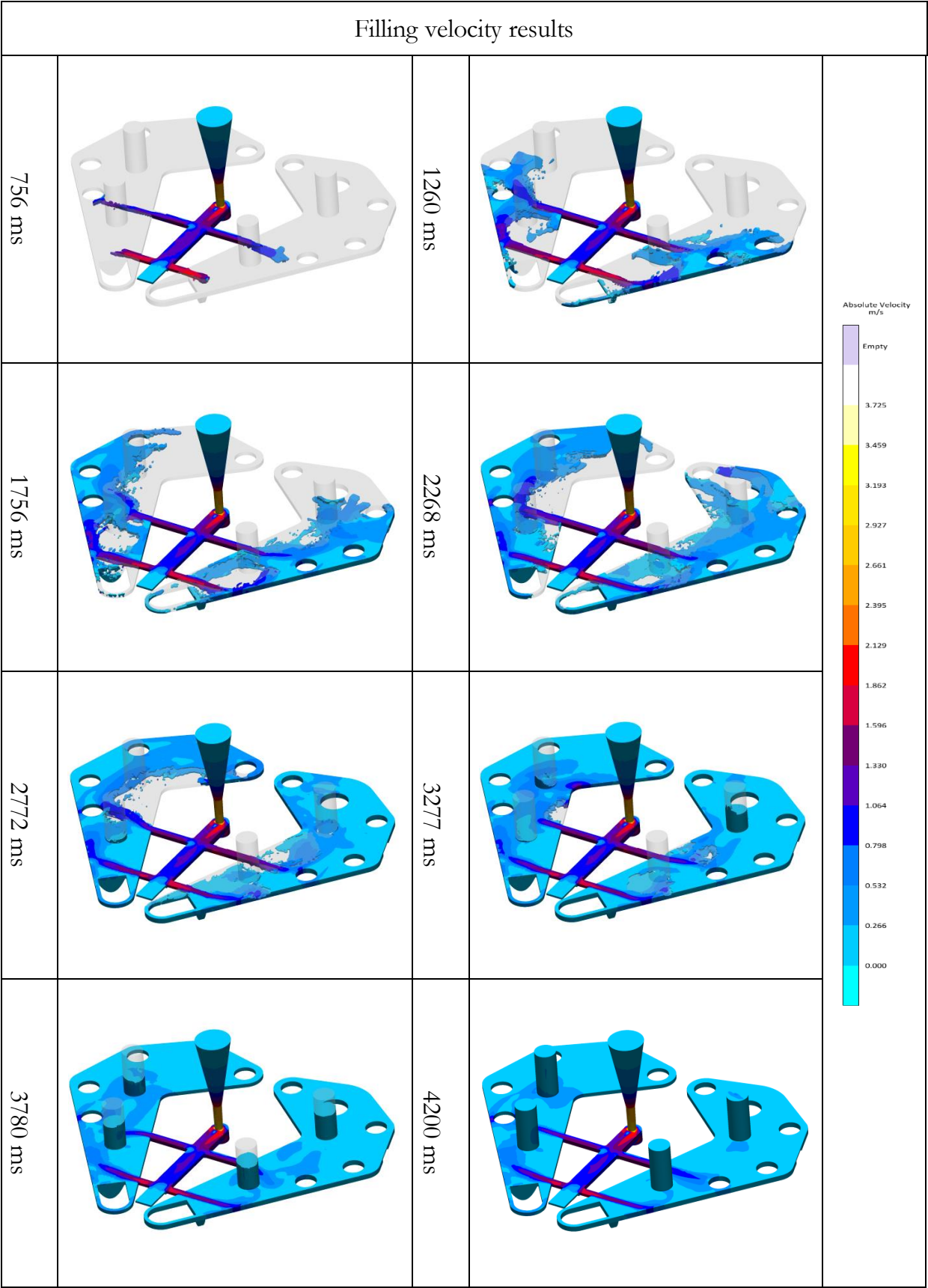


Table 8 Casting velocity simulation results using MAGMASoft 5.5.1

As it can be seen, although the ideal velocity of 0.5 m/s is overpassed, not more than 1 m/s is generally seen without considering the ingates.



## Simulations

At 1260 ms, it can be observed how the melt from both gates meet in the middle of the piece. This situation can create bifilms, that will be entrained and end up in the final piece. This situation is considered a better case scenario compared to the lack of filling if one gate is used.

Another possible defect observed from 1260 ms to 3277ms is the appearing of spaying when the center of the piece keeps being filled, which can also cause bifilms.

Another try to have a smoother flow was the use of a well to slow the melt.

As it can be seen, the melt comes down from the sprue at an approximate velocity of 4 m/s and this velocity gets reduced to approximate 1 m/s at the exit of the well.

This well also reduces the turbulent flow of the melt, decreasing the potential defects that can cause, if not used, the high velocities of 4m/s that can be reached would imply disintegration of the melt, bringing with it entrainment defects.

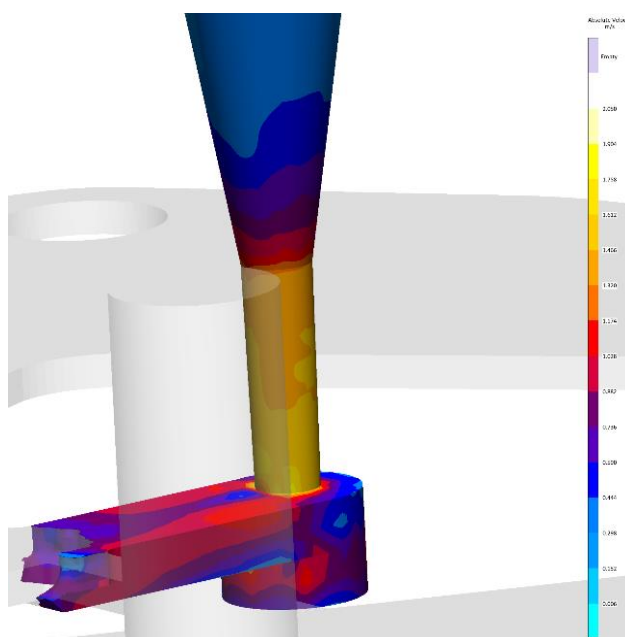


Figure 40 Well impact on the velocity

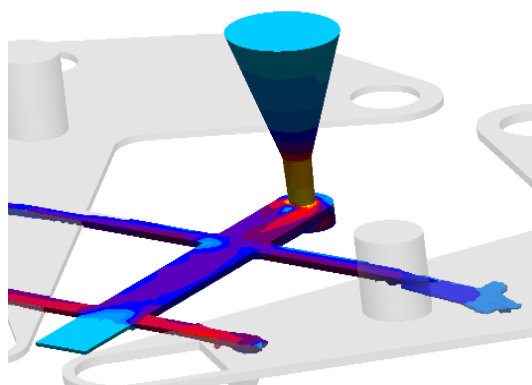


Figure 41 Ingates velocity with the first melt

Another included feature was the runner extension used to trap the first melt and prevent it from entering the chassis. It is better to avoid this first melt due to the probability of it having different defects and forming entrainments.

As it is seen on Figure 41, some of it passes through the first ingates, but most of the initial melt reaches the entrapment.

Another function of this feature was to lessen the effect of the melts impact with the end of the runner channel. This

impact could create a jerk that would introduce the melt into the cavity with even a higher velocity.

### 4.4.3.2. Solidification results

As it can be seen, the whole filling of the cast is done without a substantial decrease of temperature. As the melt was almost fully liquid at the end of the filling, as it can be seen in the following Table by the temperature, the potential for a mis-run or a cold-run was considered low.

As expected, the thinner parts such as the tensioning bracket solidify much faster than the center, which happens to be the thickest part of the piece.

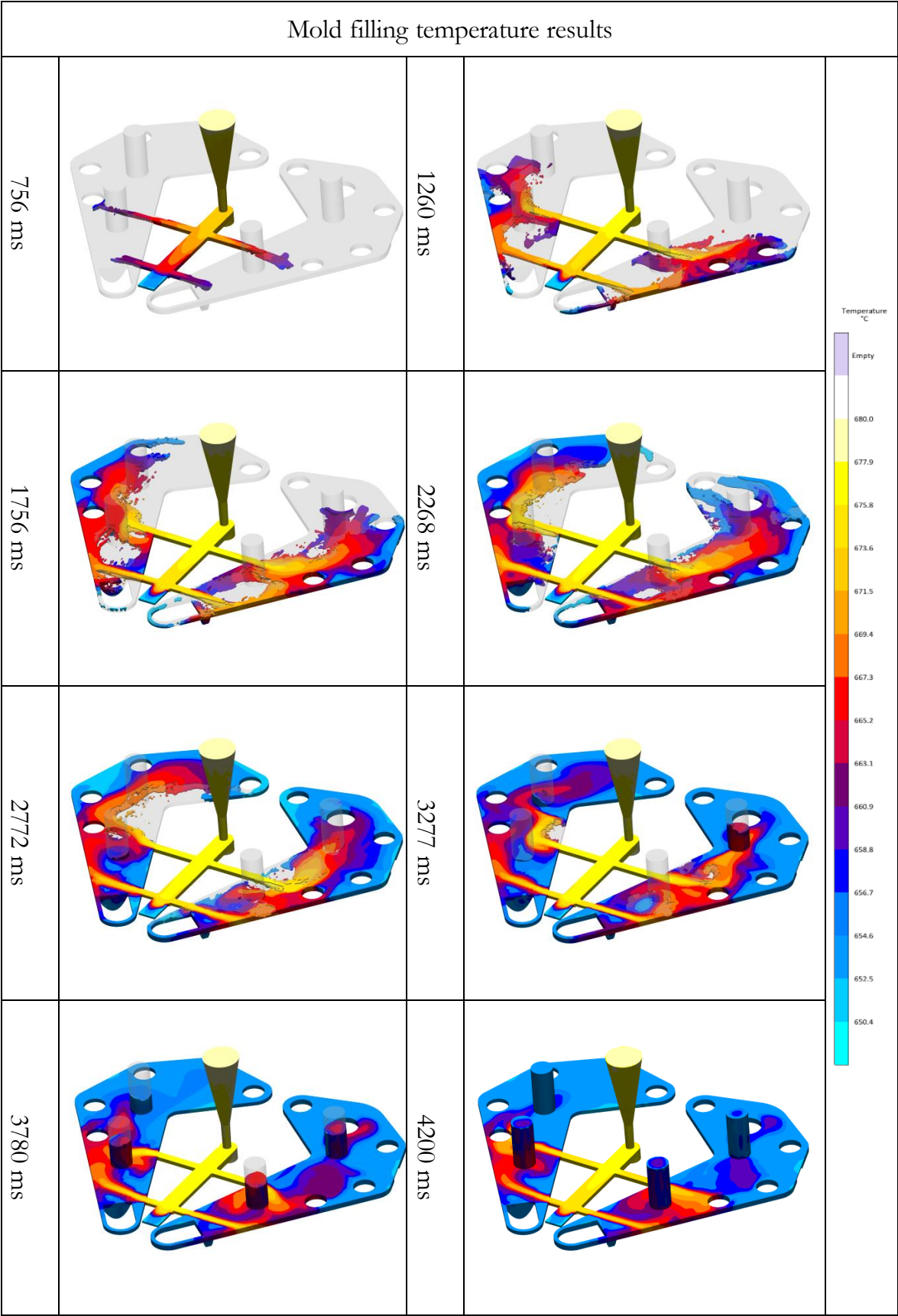


Table 9 Casting temperature simulation results using MAGMAsoft 5.5.1

As it can be seen, at the end of the filling, all the risers and the sprue, are filled with melt to the top, implying a full filling of the cast pieces.

## Simulations

However, it can be appreciated that there are some areas with noticeable higher temperature in the middle of the piece that can bring to hotspots as explained and shown in Figure 42 and Figure 43.

The location of the hotspots was expected to be where most of the mass was going to be placed, which is the thicker part of the cast. This situation could be expected due to the large area to cover and the big mass required for it.

As it is seen, those areas could be an indication of a shrinkage porosity to form and have to be thoroughly analyzed.

The porosity results that can be observed are coming from liquid shrinkage. Usually, those porosities can be solved using more ingates but this solution was discarded due to the difficulties of feeding such small part without creating more damage.

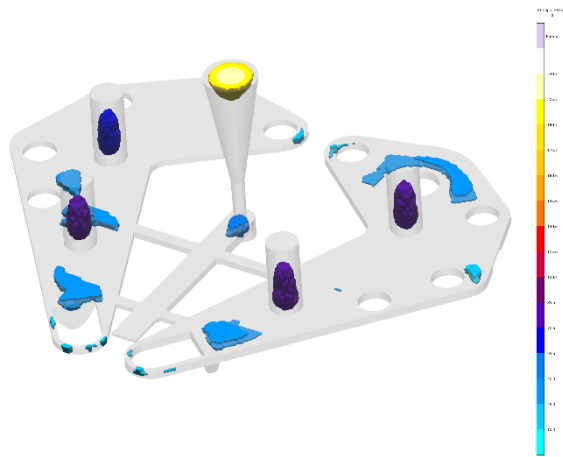


Figure 42 Hotspots locations



Figure 43 Porosity locations



## 5 Economic analysis

In this chapter, a rough estimation of the cost of both methodologies is shown. This will be one of the main reasons to decide for one of the options, considering that both models will have a similar performance.

### 5.1. CNC version cost

First, the costs of CNC machining as stated before is established. This cost is divided mostly in few aspects such as labor and machine costs, tooling, material and setup. ('How Much Does CNC Machining Cost?', 2020). This cost can be summed up in the following equation.

$$C_{CNC} = C_{material} + C_{labour} + C_{machine} + C_{setup}$$

This equation is used to calculate the manufacturing costs, without considering any fix costs, administrative, logistics or other added treatments.

#### - Material costs

This cost considers directly the raw material needed to finish the piece.

The material cost is directly both normalized aluminum sheets and the welding rod used to attach the pieces.

One piece of Aluminum of 1x1 m the 2000 series costs around 3950 SEK for the model of 12mm. To weld aluminum, we can use TIG welding with rods of approximately 100 SEK.

This leaves a cost of:

$$C_{material} = 3 \cdot 3950 + 1 \cdot 100 = 11950 \text{ SEK}$$

#### - Labor costs

This cost considers the time that an operator will have to invest in order to have the piece done.

The labor cost should be assigned to the welding time needed for a small piece like that, which is around 1 hour. The hourly wage of a welder is about 250 SEK. This leaves a cost of:

$$C_{Labour} = 1 \cdot 250 = 250 \text{ SEK}$$

#### - Machine costs

This cost accounts for the investment cost that the company made to buy the machine, and the time it will take to pay off. This cost will also include the tooling.

In this case, after using CNC Simulator pro, it gives us an estimated working time of about 2 hours each big component and 2 more for the small supports. The cost of operating a CNC machine is around 380 SEK per hour leaving an estimate cost of:

$$C_{machine} = 6 \cdot 380 = 2280 \text{ SEK}$$

#### - Setup costs

## Economic analysis

This setup costs are related to the time that the operator spends preparing the machine for that piece in particular.

The time spend depends on the batch of pieces, but it is considered to be around 10% of the working time of the machine or cycle time (*CNC Setup Time and Cycle Time Savings*, n.d.).

Following that guide, it can be said that the operator will spend around 1 hour setting up the machine, at an hourly rate of 357 SEK, leaving a cost of:

$$C_{Setup} = 1 \cdot 357 = 357 \text{ SEK}$$

These calculations leave a total cost of:

$$C_{CNC} = 11950 + 250 + 2280 + 357 = 14837 \text{ SEK}$$

### 5.2. Cast version cost

The other option to manufacture this piece is using green sand casting and postprocessing using CNC machining. This cost can be calculated using the following equation (Chougule & Ravi, 2006) that divides the costs between material, labor, energy and tooling to get a rough estimation of the cost.

$$C_{Casting} = C_{material} + C_{labour} + C_{energy} + C_{tooling}$$

As before, this equation is used to calculate the manufacturing costs only, without considering any fix costs, administrative, logistics or other added treatments such as heat treatments or coating.

#### - Material costs

In the case of casting, the material cost is divided into two groups, direct and indirect materials costs.

The direct cost implies the losses of material produced during the production with the following equation:

$$\begin{aligned} C_{Direct} &= C_{unit} \cdot w_{cast} \cdot f_m \cdot f_p \cdot f_f \\ C_{Direct} &= 20 \cdot 4.2 \cdot 1.04 \cdot 1.08 \cdot 1.04 \\ C_{Direct} &= 98.12 \text{ SEK} \end{aligned}$$

$C_{unit}$  – Cost per weight of alloy 20 SEK /kg  
 $w_{cast}$  – weight of the alloy 4.2 kg  
 $f_p$  – metal loss during pouring (1.05-1.12)  
 $f_m$  – metal loss in metling (1.01-1.07)  
 $f_f$  – metal loss in fettling (1.01-1.07)

Where all the factors taken are an average and mostly depend on the performance of the foundry used.

The indirect cost of material takes into account all the molding materials, cost of cores and other surroundings.

$$C_{Indirect} = C_{mold unit} + C_{core}$$

$C_{mold unit}$  – Cost per mold

Where:

$$C_{Mold Unit} = C_{Sand unit} \cdot w_{Mold} \cdot f_{recycle} \cdot f_r$$

$$C_{Mold Unit} = 15 \cdot 267.2 \cdot 0.4 \cdot 0.5 \cdot 1.06$$

$$C_{Core} = w_{core} \cdot C_{Sand core}$$

$$C_{Core} = 0.272 \cdot 45 \cdot 0.4$$

$$C_{Indirect} = 849.68 + 4.8 = 854.56 SEK$$

$C_{core}$  – Cost of core for a unit

$C_{Sand unit}$  – Cost of sand per kg 15 SEK/kg

$w_{Mold}$  – Weight of the sand mold

$f_{recycle}$  – Percentage of recycled sand (0.1-1.0)

$f_r$  – Factor rejected casts (1.0-1.12)

$w_{Core}$  – Volume of core sand per unit

$C_{Sand core}$  – Cost of sand core per kg 45 SEK/kg

Where the volume of the sand was calculated using a box of 650·350·750 mm minus the volume of the cast pieces and the cores, resulting in  $1.67 \cdot 10^{-1} m^3$  and a density of 1600 kg/ $m^3$  giving a weight of 267.2 kg. The cores had a volume of about  $4.6 \cdot 10^{-4} m^3$  and a density of 1700 kg/ $m^3$  leaving a weight of 0.272 kg.

From those weights, only 40% of it is the sand itself, the rest is usually moisture.

Those equations leave a total material cost of:

$$C_{Material} = C_{Direct} + C_{Indirect} = 98.12 + 854.56 = 952.68 SEK$$

#### - Labor costs

Labor costs account for the costs incurred by manual labor required by the process.

Assuming that sandcasting is a relatively slow process, we will assume a best-case scenario of 0.5 unit per hour at the same cost rate as the CNC machining operator, of about 250 SEK/h.

This leaves a cost of:

$$C_{Labour} = 2 \cdot 250 = 500 SEK$$

#### - Energy costs

The cost of energy is termed as the cost for melting the metal, which is most of the energy used. This factor depends strongly on the type of furnace used, as well as the different temperatures that we can find and the type of material used.

$$C_{Energy} = C_{unit} \cdot w_{cast} \cdot f_n \cdot f_y \cdot (E_{melt})$$

$C_{unit}$  – Cost per Kwh 1 SEK /kwh

$w_{cast}$  – weight of the alloy 4.2 kg

Where:

## Economic analysis

$$E_{melt} = C_{ps} \cdot (T_{melt} - T_{room}) + L + C_{pl} \cdot (T_{tap} - T_{melt}) \quad f_n - \text{Efficiency of the furnace (3-3.5)}$$

$$E_{melt} = 1.1 \cdot (680 - 20) + 321 + 1.15 \cdot (800 - 680)$$

$f_y$  – Overall yielding 2

$E_{melt}$  - Energy required to melt the aluminium

$C_{ps}$ -Specific heat solid state 1.1 KJ/KgK

L-Latent heat 321 KJ/KgK

$C_{pl}$ -Specific heat liquid state 1.15 KJ/KgK

This left a total cost of energy of:

$$C_{Energy} = 1 \cdot 4.2 \cdot 3.25 \cdot 2 \cdot 1188 \cdot 2.27 \cdot 10^{-4} = 7.36 \text{ SEK}$$

### - Tooling costs

Considering the low number of tools required for this process, it is decided to ignore the costs of them due to the low wear out that it will produce on them.

These calculations leave a total cost of:

$$C_{Casting} = 952.68 + 500 + 7.36 = 1460 \text{ SEK}$$

To this cost we should add another 2 hours of CNC machining to finish the housings for the roller bearing and the different holes required for assembly at a cost of 250 SEK for the operator and 380 SEK for the machine, as explained before, leaving a total of:

$$C_{Labour} = 2 \cdot 250 = 500 \text{ SEK}$$

$$C_{maachine} = 2 \cdot 380 = 760 \text{ SEK}$$

The total cost of the casting procedure ends up being:

$$C_{Casting} = 1460 + 500 + 760 = 2720 \text{ SEK}$$

## **6 Conclusion**

### **6.1 Overall**

The results of this thesis demonstrate that a viable mechanical design for the traction system of the CERNbot can be achieved.

The movable design and specifications bring a design that requires a lightweight system to move and implies the use of different motors to position the wheels and move the device. These motors will also require big reductions in order to lift the device, implying an increase of the weight.

The simulations of this device have shown that the structural requirements will be different depending on the type of wheel used and that a material such as Aluminum 2024 would be enough to hold the stresses that this piece will receive without implying a big deformation of the structure. They also showed that if we focus on one type of load, the topological optimization reaches weight savings of up to 40% without affecting its performance, going from 5.4kg to 3.3 kg. When we require to be able to use the 3 of them, the mass savings are reduced to around 25%, leaving it at about 4.2 kg.

The filling results in sand casting showed a relatively smooth filling of the structure. The use of a properly design pouring system showed a big improvement regarding the inlet speed and consequently, a reduction of defects. Solidification results showed melting being fed through the gates and the requirement of risers in order to reduce the porosity that such a big piece would have if not used. The results using casting show the possibility of having porosity in some specific places that needs to be carefully checked.

Comparing the cost of casting of this structure, it is believed that casting would result in a much cheaper option, although the initial investment for this methodology is much higher.

### **6.2. Further work**

As it is known, there's a difference between the expected outcome coming from the simulations and the physical device that we are capable of achieving. This problem is magnified when we are discussing about big pieces such as the one involved in this project.

One of the reasons of this phenomena is the accuracy that we are able to achieve in a time efficient manner, when we have to set the mesh at a relatively big size and implying that some stresses in the case of Ansys or defects in the case of MAGMAsoft, can be missed. Thus, a future trial of this device is required to ensure that it can be used successfully.

## 7 References

- [1] Abd Razak, N. A., Ahmad, A., & Rashidi, M. (2017). Investigation of pouring temperature and holding time for semisolid metal feedstock production. *IOP Conference Series: Materials Science and Engineering*, 257, 012085. <https://doi.org/10.1088/1757-899X/257/1/012085>
- [2] AL-Oqla, F. M., & Salit, M. S. (2017). 3—Materials selection. In F. M. AL-Oqla & M. S. Salit (Eds.), *Materials Selection for Natural Fiber Composites* (pp. 49–71). Woodhead Publishing. <https://doi.org/10.1016/B978-0-08-100958-1.00003-7>
- [3] *Aluminium-Copper Alloy (ISO AlCu4Mg1)*. (n.d.).
- [4] Anaheim Automation. (2015). *42Y Series—High Torque Stepper Motors*.
- [5] *ASM Material Data Sheet*. (2001).
- [6] CERN. (2020). *About CERN*.
- [7] *CERNbot | Knowledge Transfer*. (2018).
- [8] Chougule, R. G., & Ravi, B. (2006). Casting cost estimation in an integrated product and process design environment. *International Journal of Computer Integrated Manufacturing*, 19(7), 676–688. <https://doi.org/10.1080/09511920500324605>
- [9] *CNC Setup Time and Cycle Time Savings*. (n.d.).
- [10] Dawson, D. (1993). *Radiation damage to materials*.
- [11] Dieter, G. E. (1997). *Overview of the Materials Selection Process*. <https://doi.org/10.31399/asm.hb.v20.a0002450>
- [12] Engineering 360. (2015). *Light Alloys and Metals Selection Guide: Types, Features, Applications | Engineering360*.
- [13] ESAB Knowledge center. (2022). *Understanding the Aluminum Alloy Designation System*.
- [14] Ferris, T. (2020). *3 Steps to Improve FEA Models | Ansys*.
- [15] Gwyn, M. (2008). *Casting Design and Geometry*. <https://doi.org/10.31399/asm.hb.v15.a0009020>
- [16] Hasse, S. (n.d.). *Foundry—Lexicon*.
- [17] How Much Does CNC Machining Cost? (2020, April 17). *Fractory*.
- [18] John. (2021, May 6). *8 Common Types of CNC Machines Explained—MellowPine*.
- [19] Lutters, E. (2014). Product Development. In L. Laperrière & G. Reinhart (Eds.), *CIRP Encyclopedia of Production Engineering* (pp. 991–992). Springer. [https://doi.org/10.1007/978-3-642-20617-7\\_6464](https://doi.org/10.1007/978-3-642-20617-7_6464)
- [20] Materials Processing. (2016). *Shape Casting—An overview | ScienceDirect Topics*.
- [21] NANOTEC SL. (n.d.). *DB80C048030-ENM05J - Brushless DC motor | NANOTEC*.

## References

- [22] Royal Society of Chemistry. (2022). *Aluminium—Element information, properties and uses* | *Periodic Table*.
- [23] Sadayappan, K., & Elsayed, A. (2018). Sand Casting of Aluminum Alloys. In K. Anderson, J. Weritz, & J. G. Kaufman (Eds.), *Aluminum Science and Technology* (pp. 193–208). ASM International.  
<https://doi.org/10.31399/asm.hb.v02a.a0006533>
- [24] SKF. (n.d.). *Surface texture of bearing seats* | SKF.
- [25] Solar Drives. (n.d.). *Single Axis Slew Drives* | Solar Drives. Kinematics.
- [26] Tasaki, R., Seno, H., & Terashima, K. (2018). Process design and control of greensand mold press casting using estimation of metal filling behavior. *Procedia Manufacturing*, 15, 443–450. <https://doi.org/10.1016/j.promfg.2018.07.241>
- [27] Teklu, E., & Marcos, R. (2009). *ANALYSIS OF CASTING PROCESS FOR COMPLEX ELECTRONIC UNIT*. 113.
- [28] Thomas Company. (2022). *What is CNC Machining?* | *Definition, Processes, Components & More*.
- [29] Tvede, L. (2021). *The rise of the radiation protection robots*. CERN.

## **8 Search terms**

Abstract,.....	1
Background, .....	5
Concept draft, .....	24
Delimitations, .....	7
Economical analysis, .....	50
Overall, .....	54
Problem description, .....	19
References, .....	55



## 9 Appendix 1

### Track before upstairs position

The first position that will be simulated is the one happening right before the contact is produced on the upstairs position. This means that there will only be one part of the track in contact with the floor, and all the weight will rely in the back axis and the front will have an approximate angle of  $27^\circ$ .

### Boundary conditions

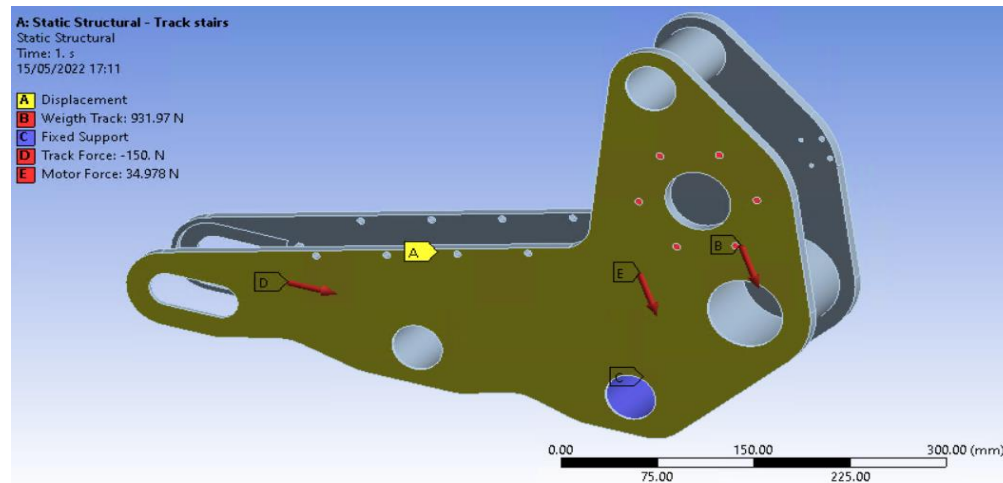


Figure 44 Boundary conditions for the track before upstairs position

To recreate the situation explained before, the following boundary conditions are applied:

- Fix the side displacement on the face attached to the robot, called A in Figure 44.
- Fix the axis that will be in contact with the floor during this position.
- The weight of the robot of 932 N in order to leave a safety factor of 1.2 considering a total payload of 620 N (64 kg) or 310 N per side. This weight is applied in the holes made for the gear reduction attached and the direction is adapted depending on the traction requirements.
- The preload applied for the track to keep the tension of 150 N in the plate that will hold the tension system.
- Traction motor weight of 35 N in the plate that will house the motor.

## Deformation

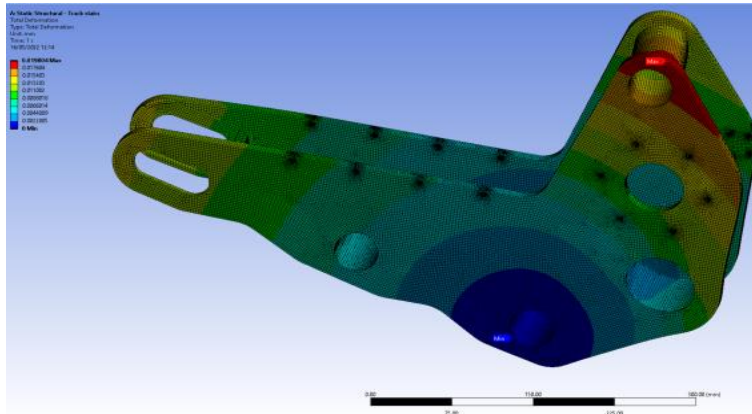


Figure 45 Track before upstairs position - Deformation simulation

As expected, the deformation increases in the upper part of the piece, where it reaches a maximum of 0.01 mm. This deformation is neglectable for the required precision. The minimum point occurs on the axis that will be fixed, leaving no deformation.

## Stress

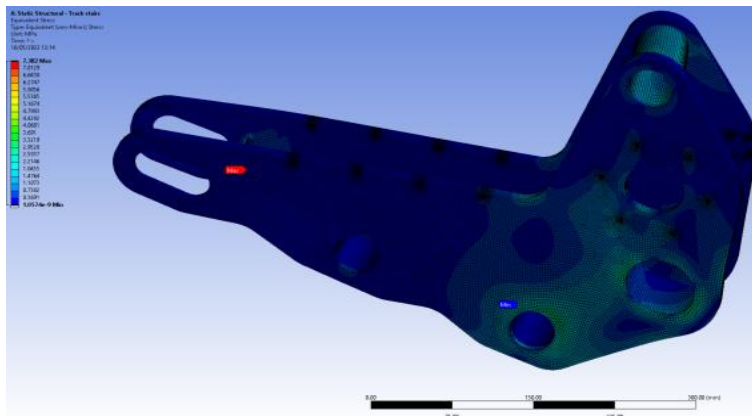


Figure 46 Track before upstairs position - Von Mises stress simulation

In the case of the stress, the maximum point is reached on the plate that will be holding the pretension required by the track. This pretension will leave a Von Mises stress of 7.4 MPa, with most of the parts of the piece that are under stress with values around 3 MPa.

## Topology optimization

### Boundary conditions

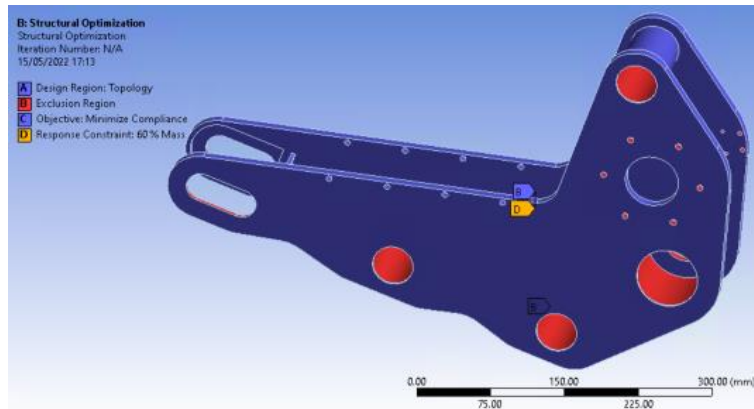


Figure 47 Track before upstairs position - Boundary conditions for topology optimization

The boundary conditions of the topology optimization take the whole piece, excluding the pieces that will require some attachment or housing (such as screws or roller bearings) and aims for a reduction of maximum 60% of the weight.

### Optimized piece

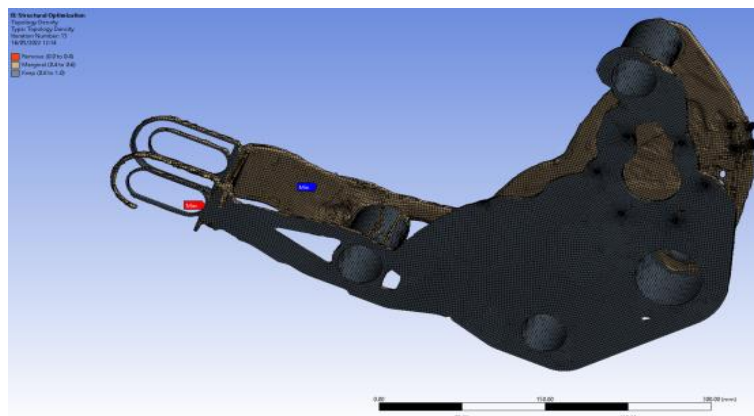


Figure 48 Track before upstairs position - Optimized piece

As it can be seen, most of the track and the mecanum-wheel parts have been reduced due to the lack of usage in this position. With this optimization, the piece weights 3.3 kg, leaving a 62.3% of the original mass.

## Pneumatic wheels

The second simulated position is the one happening when we are using the pneumatic wheel, placed on the same axis as the traction wheel for the track. This means that there will only be one axis receiving the entire load from the robot.

### Boundary conditions

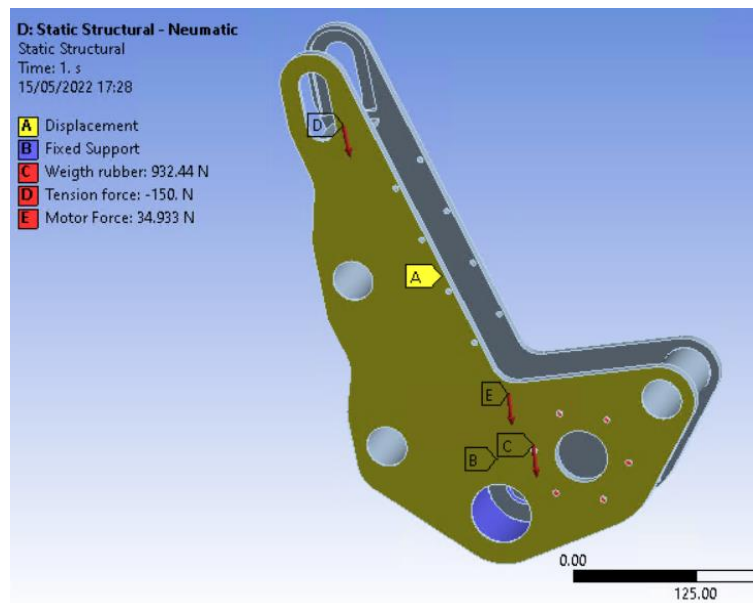
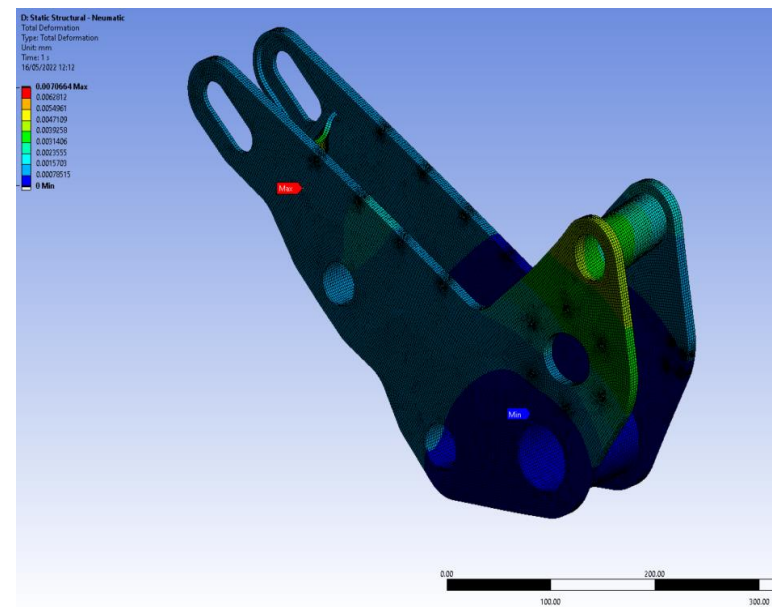


Figure 49 Boundary conditions for the pneumatic wheels position

To recreate the situation explained before, it is decided to apply the following boundary conditions:

- Fix the side displacement on the face attached to the robot, called A in Figure 49.
- Fix the axis that will be in contact with the floor during this position
- The weight of the robot of 932 N in order to leave a safety factor of 1.2 considering a total payload of 620 N (64 kg) or 310 N per side. This weight is applied in the holes made for the gear reduction attached and the direction is adapted depending on the traction requirements.
- The preload applied for the track to keep the tension of 150 N in the plate that will hold the tension system
- Traction motor weight of 35 N in the plate that will house the motor.

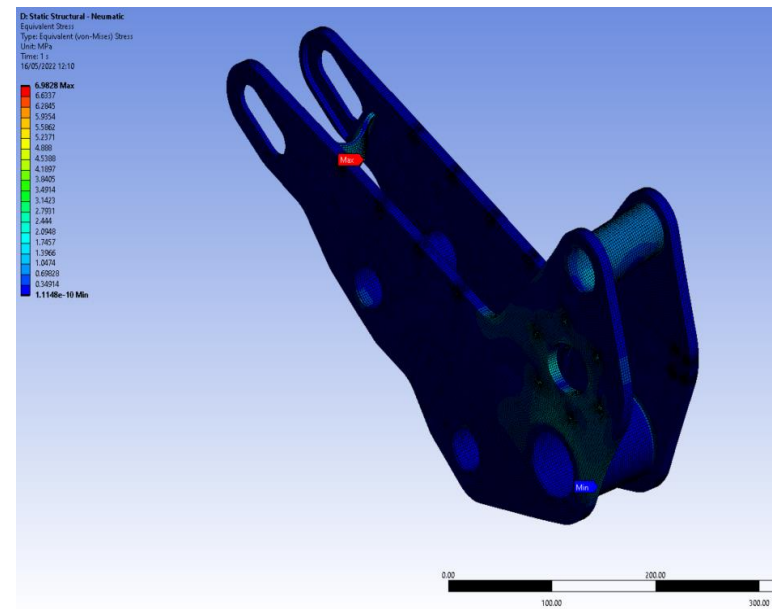
Deformation



As expected, the deformation increases again in the upper part of the piece, but this time in a much less magnitude, leaving the maximum deformation of 0.001 mm for the tension plate. The minimum point occurs on the axis that will be fixed, leaving no deformation.

Figure 50 Pneumatic wheels position - Deformation simulation

Stress



In the case of the stress, the maximum point is reached on the plate that will be holding the pretension required by the track. This pretension will leave a Von Mises stress of 7 MPa, with most of the parts of the piece that are under stress with values around 2 MPa.

Figure 51 Pneumatic wheels position - Von Mises stress simulation

## Topology optimization

### Boundary conditions

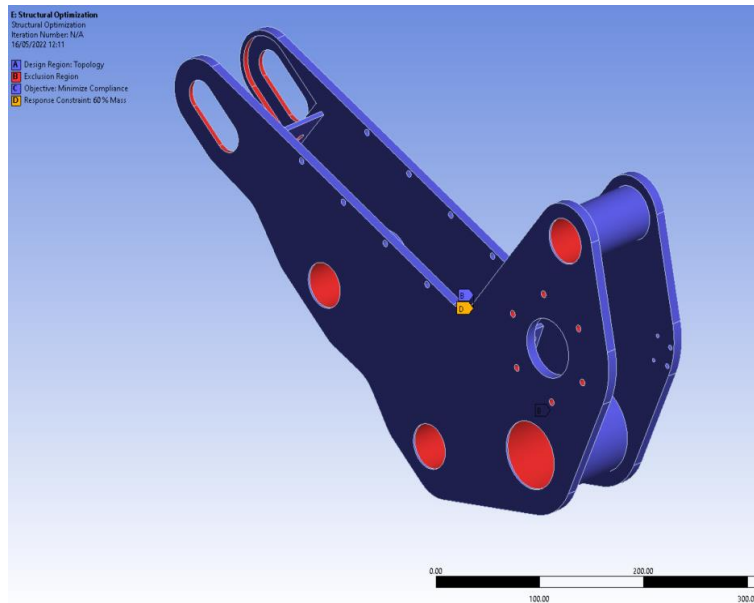


Figure 52 Pneumatic wheels - Boundary conditions for topology optimization

The boundary conditions of the topology optimization take the whole piece, excluding the pieces that will require some attachment or housing (such as screws or roller bearings) and aims for a reduction of maximum 60% of the weight.

### Optimized piece

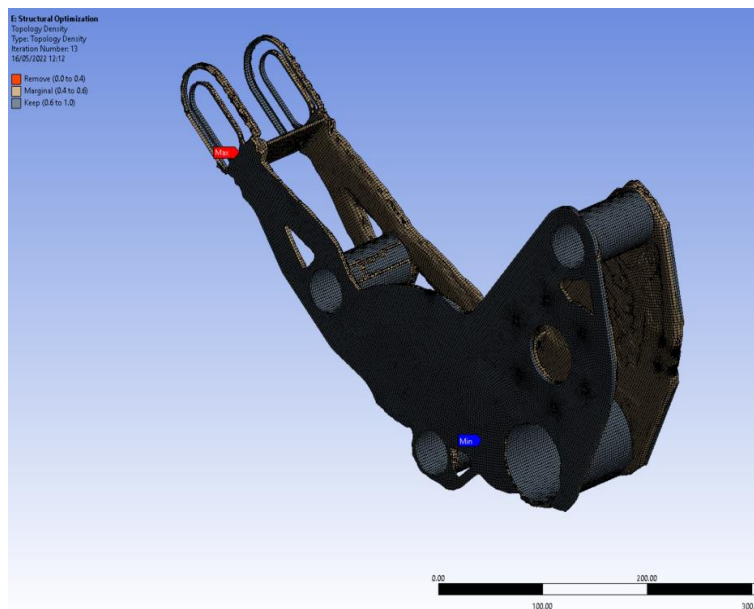


Figure 53 Pneumatic wheels position - Optimized piece

As it can be seen, most of the track and the mecanum-wheel parts have been reduced due to the lack of usage in this position but the walls of the piece kept almost intact. With this optimization, the piece weights 3.4 kg, leaving a 62.4% of the original mass.



## Mecanum-wheels

The third simulated position is the one happening when we are using the mecanum-wheels, placed on the further axis, and fed with a tension belt. This means that there will only be one axis receiving the entire load from the robot.

### Boundary conditions

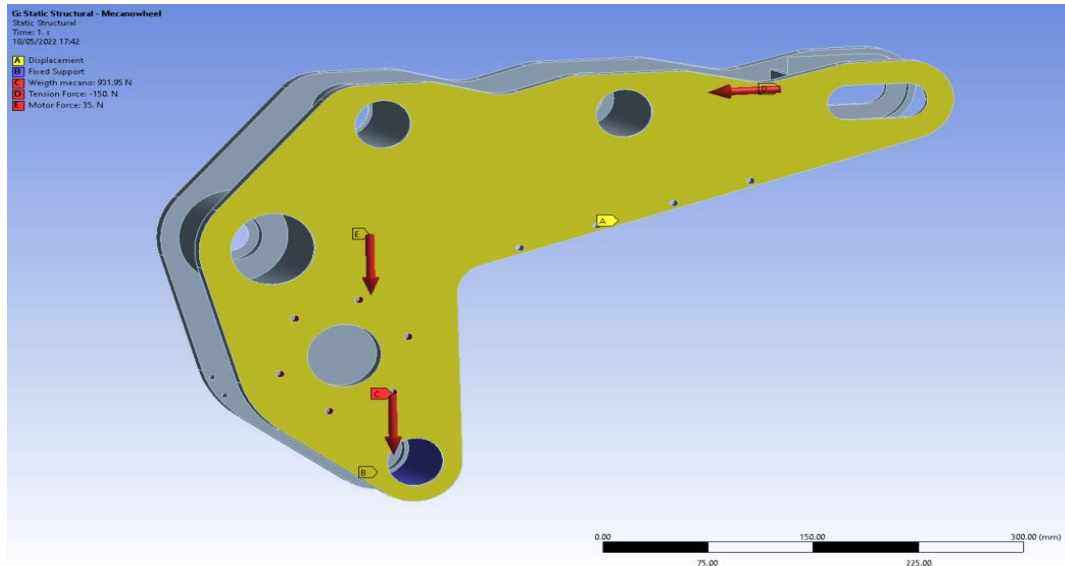


Figure 54 Boundary conditions for the mecanum- wheels position

To recreate the situation explained before, it is decided to apply the following boundary conditions:

- Fix the side displacement on the face attached to the robot, called A in Figure 54.
- Fix the axis that will be in contact with the floor during this position
- The weight of the robot of 932 N in order to leave a safety factor of 1.2 considering a total payload of 620 N (64 kg) or 310 N per side. This weight is applied in the holes made for the gear reduction attached and the direction is adapted depending on the traction requirements.
- The preload applied for the track to keep the tension of 150 N in the plate that will hold the tension system
- Traction motor weight of 35 N in the plate that will house the motor.

## Deformation

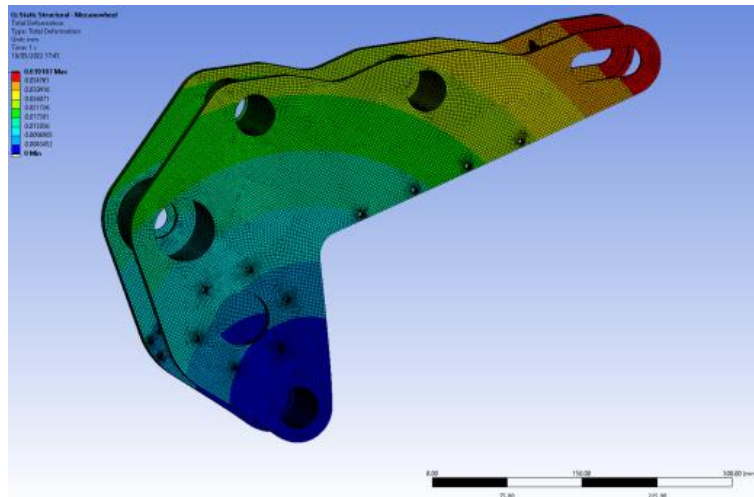


Figure 55 Mecanum-wheels position - Deformation simulation

This time, the deformation increases its magnitude due to the distance between the fixed point and the maximum deformation. This maximum deformation occurs in the upper part of the piece, reaching 0.04 mm, being an acceptable magnitude. The minimum point occurs on the axis that will be fixed, leaving no deformation.

## Stress

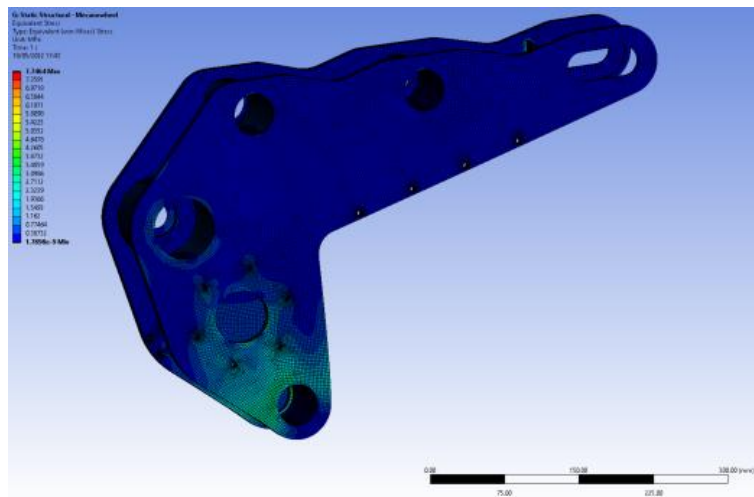


Figure 56 Mecanum-wheels position - Von Mises stress simulation

In the case of the stress, the maximum point is on the axis where the entire load is applied. All the weight will leave a Von Mises stress of 7.4 MPa, with most of the parts of the piece that are under stress with values around 1 MPa.



## Topology optimization

### Boundary conditions

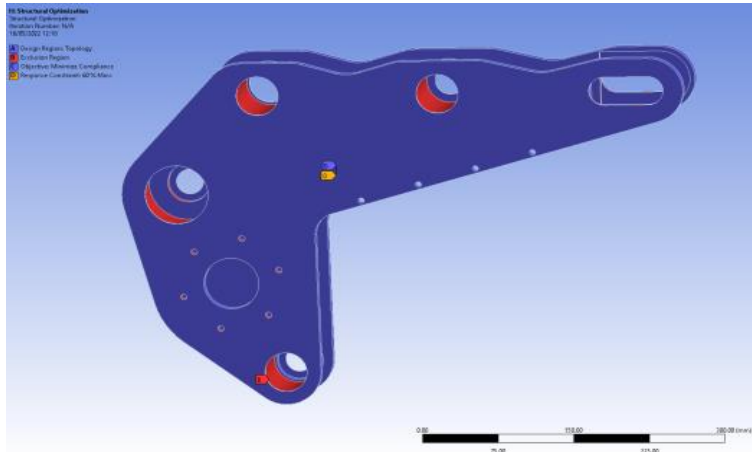


Figure 57 Mecanum-wheels - Boundary conditions for topology optimization

The boundary conditions of the topology optimization take the whole piece, excluding the pieces that will require some attachment or housing (such as screws or roller bearings) and aims for a reduction of maximum 60% of the weight.

### Optimized piece

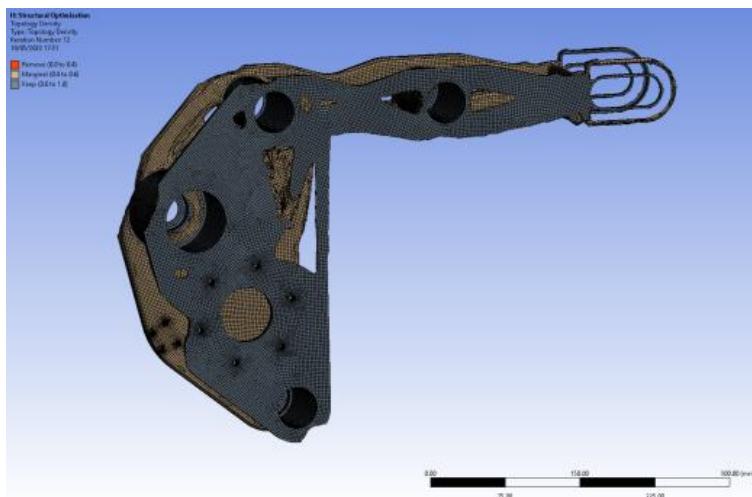


Figure 58 Mecanum-wheels position - Optimized piece

As it can be seen, most of the system has been reduced due to the lack of usage in this position. With this optimization, the piece weights 3.2 kg, leaving a 62.2% of the original mass.

## Track on the stairs

The last simulated position is the one happening when we are using the track in the stairs, meaning that the load relies on the tip of the system as shown during the calculations. This means that the entire load will be placed on the front axis.

### Boundary conditions

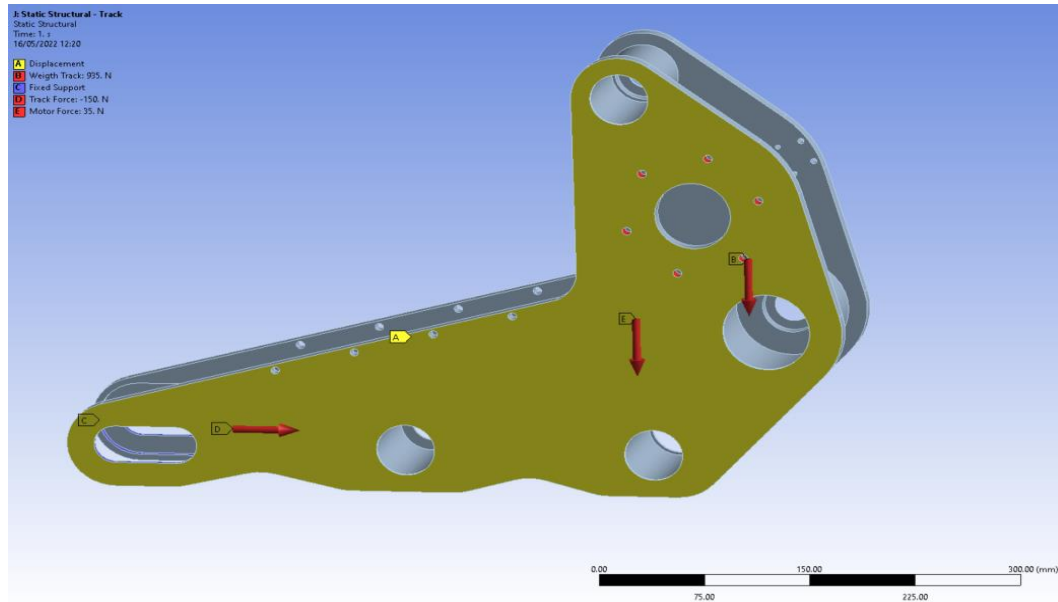


Figure 59 Boundary conditions for the track on the stairs position

To recreate the situation explained before, it is decided to apply the following boundary conditions:

- Fix the side displacement on the face attached to the robot, called A in Figure 59.
- Fix the axis that will be in contact with the floor during this position, in this case the front slot for the tensioning system.
- The weight of the robot of 932 N in order to leave a safety factor of 1.2 considering a total payload of 620 N (64 kg) or 310 N per side. This weight is applied in the holes made for the gear reduction attached and the direction is adapted depending on the traction requirements.
- The preload applied for the track to keep the tension of 150 N in the plate that will hold the tension system
- Traction motor weight of 35 N in the plate that will house the motor.

## Deformation

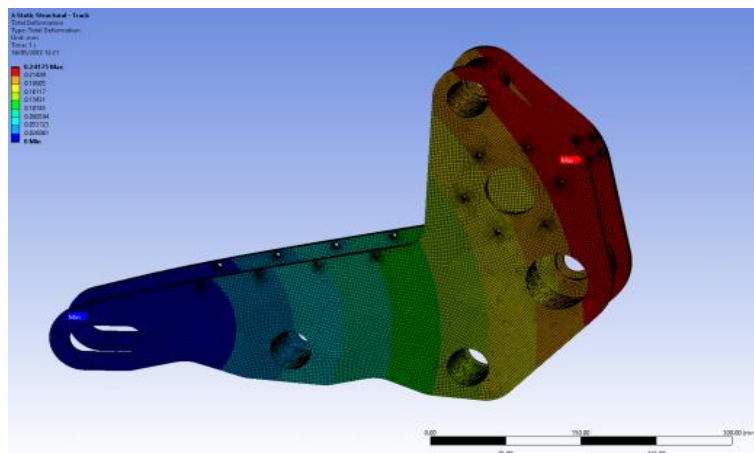


Figure 60 Track on the stairs position - Deformation simulation

As expected, the deformation in the upper part of the system has a bigger magnitude that before, due to the distance applied to it. The maximum is of 0.24 mm, still an acceptable magnitude. The minimum point occurs on the axis that will be fixed, leaving no deformation.

## Stress

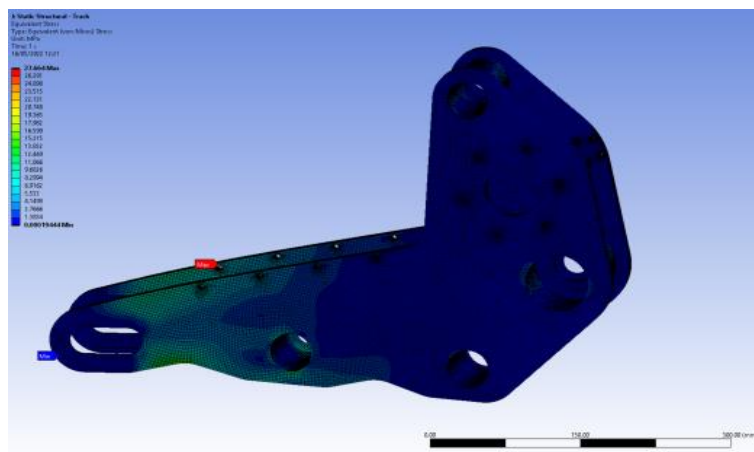


Figure 61 Track on the stairs position - Von Mises stress simulation

In the case of the stress, the maximum point is reached in a screw placement for a cover that will be applied afterwards. This maximum stress will reach 27.6 MPa. Most of the parts of the piece that are under stress with values around 5 MPa, mostly on thinner sections due to axes placement.

## Topology optimization

### Boundary conditions

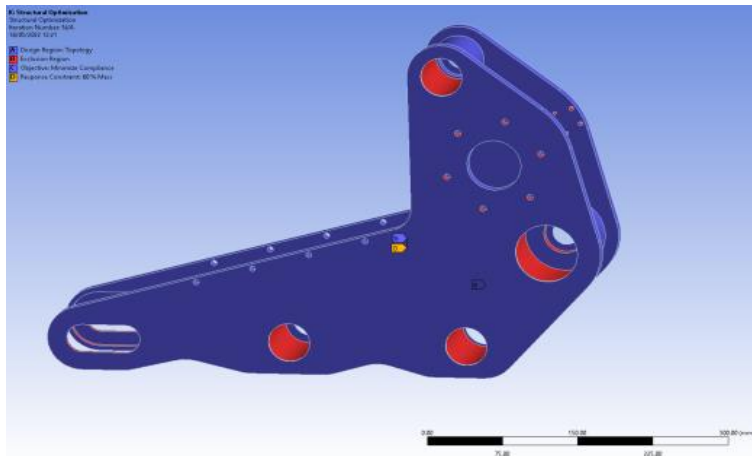


Figure 62 Track on the stairs position - Boundary conditions for topology optimization

The boundary conditions of the topology optimization take the whole piece, excluding the pieces that will require some attachment or housing (such as screws or roller bearings) and aims for a reduction of maximum 60% of the weight.

### Optimized piece

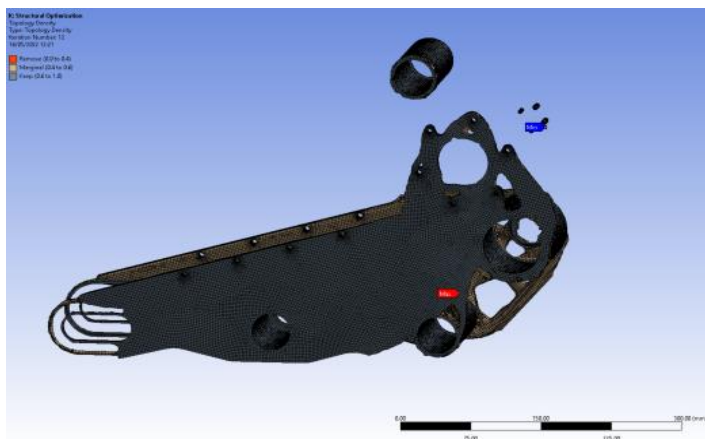


Figure 63 Track on the stairs position - Optimized piece

As it can be seen, most of the mecanum-wheel parts have been reduced due to the lack of usage. With this optimization, the piece weights 3.3 kg, leaving a 62.3% of the original mass.